Modeling Inlet Hydraulic Performance Using the Storm Water Management Model

by

Larissa da Costa, BSCE

A Thesis

In

CIVIL ENGINEERING

Submitted to the Graduate Faculty
of Texas Tech University in
Partial Fulfillment of
the Requirements for
the Degree of

MASTER IN SCIENCE

IN

CIVIL ENGINEERING

Approved

Theodore G. Cleveland, Ph.D., P.E.
Chair of Committee

Annette Hernandez, Ph.D.

Peggy Gordon Miller
Dean of the Graduate School

August, 2011

ACKNOWLEDGMENTS

I would like to thank my family and friends, Jose da Costa, Vilma da Costa, and Raissa da Costa, for all the love, support and patience during these past few years. I would like to recognize Andrea Campos and Carlos Zepeda for helping with figures and checking calculations for my work.

Special thanks should be given to my student colleagues who helped in many ways. Starting with the laboratory manager, Wade Barnes, for keeping everyone on task and the experiments going, and the data collection team composed of graduate students, Martin Aziz and Bijay Basnet and undergratuate students, Zeferino (Nino) Mendoza, Holly Murphy, Janice Rainwater, Kirsten Singleton, and Annabell Ulary for all their patience and hard work during the summer of 2009.

I would like to thank the Water Resources Center Director Kenneth Rainwater, PhD, PE for allowing me into the masters program and thank the Water Resources Center under the Civil Engineering at Texas Tech University for allowing me to work with the data from the projects.

I would like to express my gratitude to the committee chair and advisor Theodore Cleveland, PhD, PE for all the help and guidance during the thesis process, and my committee member Annette Hernandez, PhD for all the support provided during the thesis completion.

Finally, I would like to thank the Texas Department of Transportation (TxDOT) for financial support provided by the research projects 0 – 5823, 0 – 6070, 0 – 6358, in particular 0 – 5823 which is the subject of this thesis.

TABLE OF CONTENTS

LIST OF TABLES

LIST OF FIGURES

ABSTRACT

The Texas Department of Transportation (TXDOT) uses Type–H inlets as a median drain for divided highways and as lateral drains on feeder roads. The Federal Highway Administration (FHWA) manual presents the hydraulic aspects of drop–type median inlets. These inlets are usually designed using empirical equations, that are time consuming, propagate rounding errors, and have multiple solutions.

One of the solutions for such problems is the use of a modeling program to attempt to simulate drop–type inlets. The modeling was performed using over 250 physical experiments conducted on Type–H inlets at Texas Tech University. The experiments were performed in an 8 feet wide by 48 feet long flume, with tiltable slopes of 0.5%, 1.0%, and 2.0%.

The U.S. Environmental Protection Agency (EPA) Storm Water Management Model (SWMM) was used to explore the ability of the program to simulate drop–type inlets. The methodology describes the physical models and how the drop–inlets were conceptualized and then modeled in SWMM. The results of the modeling effort found that the simulated values were within 2.0% of the observed values for the approach flow and outflow of the inlet, but could not predict depths well. SWMM can perform adequately for use in designing Type–H inlets with minimum input information, with the caveat that the depth predictions are poor. Future work should include different types of inlets to test the methodology, and refinement of the modeling technique to more accurately predict flow depths.

CHAPTER 1
INTRODUCTION

The Texas Department of Transportation (TxDOT) uses Type–H inlets as a median drain for divided highways and as lateral drains on feeder roads. These inlets are traffic-safe, a requirement that dictates geometric aspects of their design. These inlets are illustrated in TxDOT specification sheets appendix-I in Cleveland, et al. (2010). Figure 1 shows a Type–H inlet in service.

Figure 1: Type-H inlet located on I-35 feeder near San Marcos, Texas.

Federal Highway Administration (FHWA) Hydraulic Engineering Circular 22 (HEC22) manual discusses the hydraulic aspects of generic drop–type median inlets. Despite these manuals, inlet design is complex. Engineers have to balance inlet flow capacity, inlet location, and inlet maintenance, as part of the design process. One challenge of design is modeling inlet behavior in a typical hydraulic model so that arrays of inlets may be examined.

In the summer of 2009, Texas Tech University examined models morphologically similar to Type–H inlets. These experiments examined flows at three different slopes using a combination of vault boxes to determine the hydraulic behavior of the inlet. The experimental program produced over 250 unique experiments. Details of the experimental program can be found in Cleveland, et al. (2010).

The Environmental Protection Agency (EPA) Storm Water Management Model (SWMM) is a program that can be used to model flow through open conduits and pipes in a system; this thesis examines the effectiveness of the SWMM program in modeling the Type–H inlet.

The objective of this thesis is to evaluate SWMM as a tool to be used to design systems of such inlets, and provide some guidance of how to model the inlets on SWMM.

CHAPTER 2
LITERATURE REVIEW

This review investigated papers on different modeling scenarios for stormwater flow, the accuracy of scale models as well as the accuracy of modeling software, and modeling software in general.

2.1 Prior Experimental Studies

Larson (1948) reported on a comparatively early study of grate inlets with free drops beneath the grate. The experiments were conducted at the Saint Anthony Falls Hydraulic Laboratory of the University of Minnesota. The research experimentally examined gutter inlets with different grate types. The researcher concluded that the width of the inlet normal to the direction of the flow and the efficiency of the inlet opening have the most influence in determining the capacity of the inlet.

Li, et al. (1954) examined the hydraulic behavior of depressed combination inlets. The models used had a 1:3 scale. Five different inlets were tested in combination. The study focused on the effects on inlet efficiency of the following factors:

1. Type of grate, and
2. Position of the grate relative to the curb opening.

Several conclusions were drawn from the study. In relation to the position of the grate relative to the curb opening the most efficient designs were those with fewer transverse bars. the only exception being when placed upstream of the curb opening. Using a more efficient grate and moving the inlet upstream or downstream of the curb opening, there was a significant increase in the inlet efficiency. Lastly, an increase in capacity can be achieved by placing the grates with transverse bars directly upstream or downstream of the curb opening.

Cassidy (1966) examined five types of grate inlets in six different geometries. A relationship was found relating the flows and the depth and width of the inlet. The research suggests that the spacing and proportioning of the inlet is related to the relative depth and the Froude number. Cassidy's work was a design guidance approach with emphasis on relating dimensionless quantities with inlet performance.

Argue and Pezzanti (1996) conducted 4:10 scale model experiments on curb inlet called a "Bro–Pit". Figure 2 is a sketch of the "Bro–Pit" inlet.

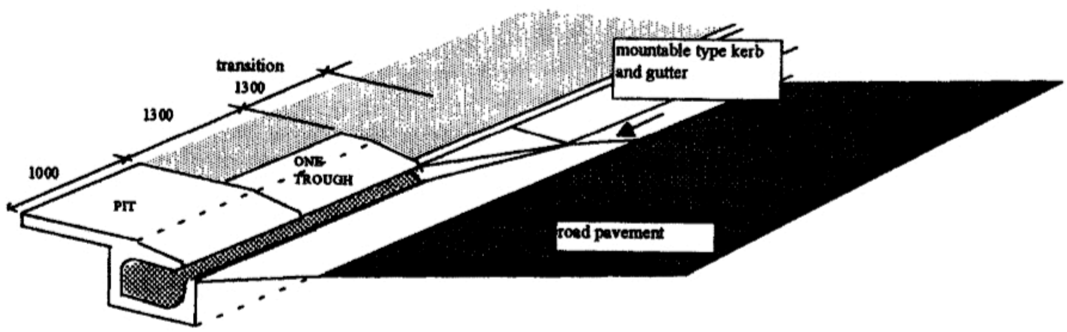

Figure 2: Bro-Pit inlet representation (Argue and Pezzanti, 1996).

The inlet is comprised of different components for a pit set behind the curb alignment. The results showed that there was up to 40% significant difference in the flow being captured. The full size model performance improves as the flow increases and the transition zone for the turbulent regime decreases. Morphologically the Bro – Pit is a capped Type–H with 3 sides blocked.

Bobde (2007) conducted a literature review on drop–type inlets as part of the Type–H research. He attempted to extend Cassidy's concept of relating geometric ratios and dimensionless numbers as performance predictions and conducted exploratory work using regression analysis to develop an analytical framework for interpreting experimental results.

The Texas Department of Transportation funded an extension to the afore-mentioned research project which performed experiments on Type–H inlets and analyzed the hydraulics of such inlets. Texas Tech University conducted the experiments. There were 274 physical models tested. The experiments were reproduced for three different slopes (0.5 %, 1.0 %, and 2.0 %) and different vault boxe sizes. Three sizes of vault boxes were used, 1 feet x 1 feet, 2 feet x 2 feet, and 2 feet by 4 feet, with different sizes of inlets (4 inches, 8 inches, and, 12 inches).

Further information can be found on Technical Report Hydraulic Capacity of Type–H Inlets by Cleveland et al., (2010).

2.2 Modeling Approaches

Urbonas (2007) examines each issue and whether modeling is a good or bad representation of the real world. The issues that were addressed include continuous simulation, design storms, temporal and spatial rainfall data density in continuous simulations, aerial corrections for modeling larger catchments and other challenges from modeling. The accuracy of the model is connected to a lot of factors. For a successful model, the most important factor is the knowledge and skills of the modeler. The modeler needs to be well versed on the available software in order to choose the best one for modeling. Each software has its limitations when dealing with modeling equations.

The Harvard Gulch catchment was used as an example on how to "handle" the issues addressed in Urbonas (2007). The Harvard Gulch catchment was modeled in EPA SWMM in kinematic mode. Each element was set up to have an overflow when the design capacity was reached and the excess flow was routed to the streets or adjacent floodplains. The author concluded that a good computer model is highly dependent on the expertise of the modeler and/or the team doing the modeling.

The U.S. Department of Transportation–Federal Highway Administration, Hydraulic Engineering Circular No. 22 (HEC–22)–Urban Drainage Design Manual, provides the initial guideline in chapter 4 for the selection and design of drop–type inlets. While the design guidance was found to be adequate in the Type–H study, there was no guidance of how to incorporate the inlet into an integrated hydraulic model to design drainage systems. Each inlet in HEC–22 approach is independent while in real systems there is undoubtably interactions between inlets, the drop–vault and the subsurface storm sewer system.

Houston Storm (HouStorm) is an extension from TxDOT WinStorm. The software is used in Houston, Tx to design storm drainage systems for a drainage network using drainage areas, nodes and links. The program does not directly allow for inlet modeling (WINSTORM, 2008).

The U. S. Environmental Protection Agency (USEPA), Storm Water Management Model (SWMM) is an integrated hydrologic–hydraulic program that can model flow through open conduits and pipes in a system. This thesis examines the ability of SWMM to successfully model Type–H inlet.

CHAPTER 3
METHODS

This chapter briefly describes the experimental methods used in the Type–H physical model experiments and the representation of these real physical models in the SWMM computer program. The methods to analyze the experiments use SWMM as a hydraulic model and experiment with different elements (weirs) and compare the results to the physical model. A brief description of the physical model follows.

The author was one of several research assistants that built the physical model experiments and collected measurements, while the SWMM modeling in this thesis is the author's unique contribution to the overall understanding of drop–inlet design.

3.1 Physical Model Experiments

A tiltable, recirculating aluminum flume 8 feet wide by 48 feet long with glass panel sides was used for a series of inlet physical models experiments. The glass panels allowed cameras to be positioned outside of the flume to record interesting behavior. Figure 3 shows the channel set for the experiment.

Figure 3: Flume with the experimental model installed.

Three longitudinal slopes were used for the physical experiments to represent various kinds of vertical curvature anticipated in median drainage cases. The three experimental slopes were 0.5%, 1.0%, and 2.0%. These conditions were replicated in the Stormwater Management Modeling (SWMM) simulations.

3.2 Inlet Physical Models

The physical model was built of wood inside the flume. The cross-section was a trapezoid section. The width of the channel bottom was two feet with 6:1 (H:V) side slopes. The inlet was located at the downstream end of the flume at approximately 35 feet from the upstream outfall. A ½ foot tall by eight feet wide ditch block, shown in figure 4, was installed. The ditch block was sloped towards the inlet hole. Experiments were performed with and without the ditch block in place. The ditch block mimics a Federal Highway Administration (FHWA) design guideline to increase the capture of a median inlet.

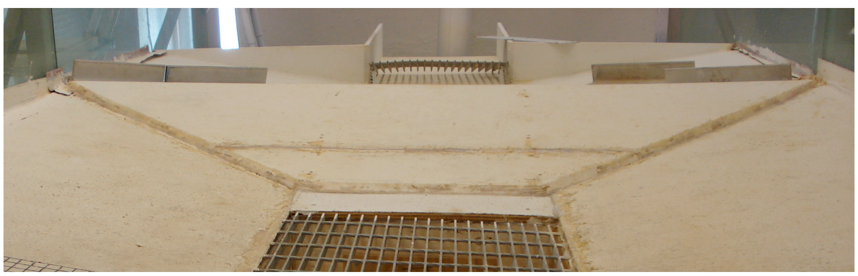

Figure 4: Ditch block set-up.

Water leaves the median ditch system two ways: captured by the inlet, and/or as overflow. Downstream of the ditch block, a two feet wide overflow channel extended to the end of the flume. This overflow channel was used to capture the flow beyond the inlet to quantify uncaptured flow.

A subsurface drain pipe carried captured flow away from the inlet. The drain was a 1 foot diameter pipe that tilted with the model. A riser pipe was cut into the drain as an independent measurement of captured flow.

On the subsurface drainpipe a six inch hole was cut and a six inch riser was installed. The six inch riser measured the flow captured by the inlet. Figure 5 shows the overflow channel, the backsplash and the six inch pipe.

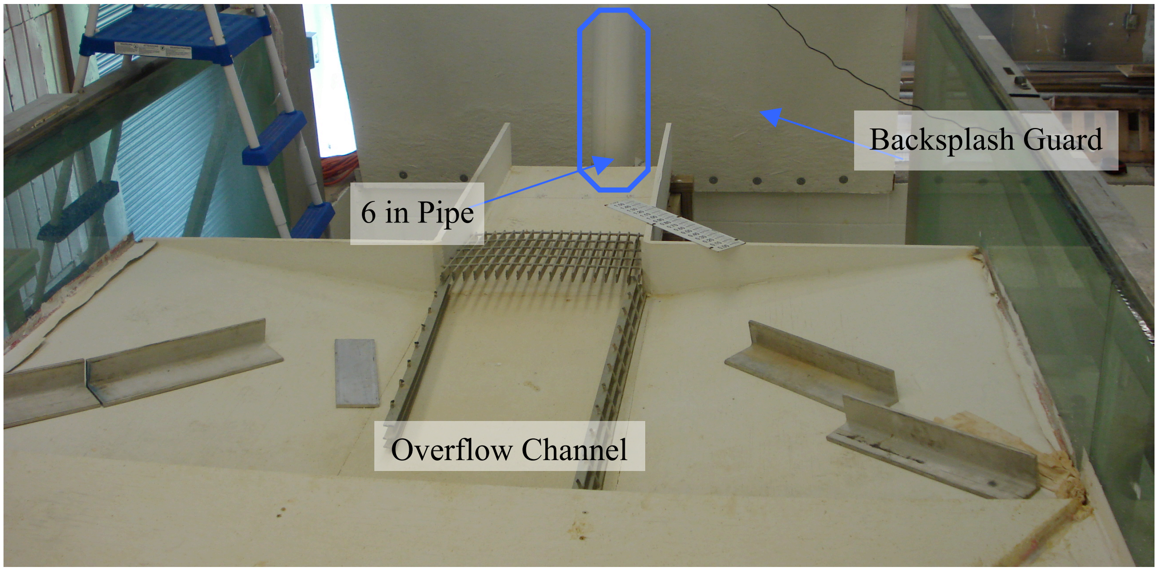

Figure 5: Overflow channel, backsplash, and the 6 inch pipe.

Five different configurations were studied generating 274 different experiments. The outlets sizes ranged from four inches to 12 inches and were positioned on the bottom and top of the boxes. The box sizes were 1 feet x 1 feet, 2 feet x 2 feet, and 2 feet x 4 feet for single boxes. The tandem case (figure 6b) had 2 boxes 1 feet x 1 feet connected by eight inches pipe. Figure 6 is a collection of images of the vault boxes.

(a) (b)

Figure 6: Inlet set-up for (a) single and (b) tandem boxes.

The median ditch model was painted with a mixture of sand and paint to simulate the friction of concrete. The paint was rolled and sand was applied and allowed to set overnight.

The first experimental set–up tested the orientation of the grate as well as the open hole (no grate). The inlet grate was placed parallel and perpendicular to the direction of the flow. The orientation of the grate in relation to the flow had no measurable difference, so later experiments were run in a parallel set–up (Cleveland, et al., 2010)[1]. Table 1 lists the combinations of inlet and outlet set–up.

Table 1: Configuration for the experiments.

Inlet	Grate	Outlet Set-up				
1’ x 1’ - 1	No Grate	4 - Low	4 - High	8 - Low	8 - High	N/A
1’ x 1’ - 1	Parallel	4 - Low	4 - High	8 - Low	8 - High	N/A
1’ x 1’ - 1	Perpendicular	4 - Low	N/A	8 - Low	8 - High	N/A
1’ x 1’ - 1	Parallel - No Ditch Block	4 - Low	4 - High	8 - Low	8 - High	N/A
1’ x 1’ - 1	Parallel - Rear	4 - Low	N/A	8 - Low	N/A	N/A
1’ x 1’ Tandem	No Grate	N/A	N/A	8 - Low	N/A	N/A
1’ x 1’ Tandem	Parallel	4 - Low	4 - High	8 - Low	8 - High	N/A
1’ x 1’ Tandem	Perpendicular	N/A	N/A	8 - Low	N/A	N/A
1’ x 1’ Tandem	Parallel - No Ditch Block	4 - Low	4 - High	8 - Low	8 - High	N/A
2’ x 2’ - 1	No Grate	N/A	N/A	8 - Low	N/A	12 - Low
2’ x 2’ - 1	Parallel	4 - Low	N/A	8 - Low	N/A	12 - Low
2’ x 2’ - 1	Lid	4 - Low	N/A	8 - Low	N/A	12 - Low
2’ x 2’ – 1	Parallel - No Ditch Block	4 - Low	N/A	8 - Low	N/A	12 - Low
2’ x 4’ – 1	Parallel	4 - Low	N/A	8 - Low	N/A	12 - Low

[1] Also, the inlet performed as well with a grate as without one, the experiments were discontinued as the experiments progressed, because in practice open hole systems are not intentionally used.

3.2.1 Data Collection Stations

Data was acquired at several cross sections along the median ditch using video imaging and various measurement tools. The video image stand locations are shown in Figure 7 along with the platform locations.

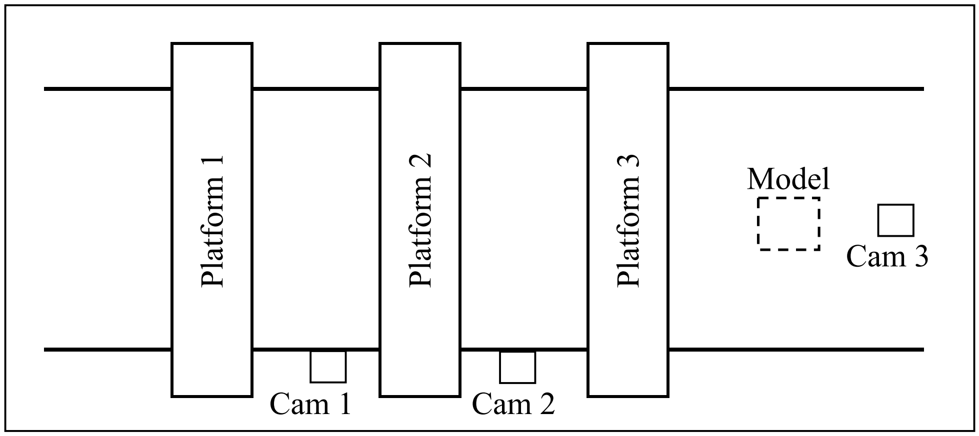

Figure 7: Platforms and camera positions.

3.2.2 Platform Measurements (Tools and Techniques)

Lines were drawn longitudinally along the flume, from right bank to left bank at 1/2 foot increments to create the 5 stations on the channel (the "straight" part of the flume). Each time a measurement was made it was made at the same station to ensure that data collection was consistent. Figure 8 shows the 5 stations along the channel.

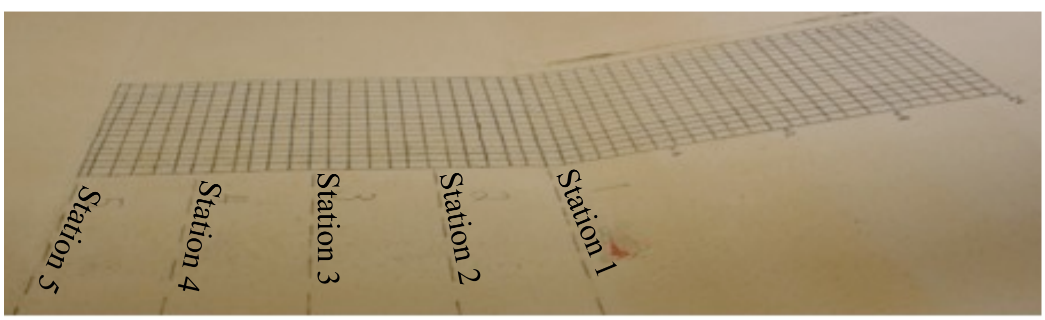

Figure 8: 5 Stations along the channel.

3.2.3 Instruments

This section summarizes the instruments used for the collection of the data. Instrumentation detail is contained in appendix A.

Staff gages were used to measure depth. The staff gage used was a plumb bob at the end of a metal rod. The rigid metal rod had markings at every 0.10 feet. The plumb bob was positioned to just the water surface elevation and the distance was read. The difference of this reading and distance to the channel is the flow depth at the particular location.

A SonTek® Flowtracker Acoustic Doppler Velocimeter (ADV) was used to find discharge across the channel. The ADV measures current in 2-Dimensional/ 3- Dimensional. The sampling volume is cylindrical located about 10.0 centimeters (4.0 inches) from the probe. The transmitter generates a sound that bounces off the suspended particle in the water. The sound returns to the receiver and is averaged together by the processor to infer a velocity from the doppler shifts at the return signal. The instrument measures velocities as low as 0.001 meters/second (0.003 feet/second) to as high as 4.0 meters/second (13 feet/second). It can measure velocities at a depth as shallow as 2.0 centimeters (0.78 inches). The user inputs the location and depth and the instrument calculates the area and discharge. Although the ADV has the ability to calculate discharge, a second instrument, a small “price–type” current meter (typically called a pigmy meter), was used when the flow depth was lower than 2.0 centimeters (0.78 inches).

The Pigmy is a current meter with cups located on the base that resemble an anemometer. It measures velocities by counting the number of revolutions in a period of time. The pigmy was used when the flow depth was lower than 2.0 centimeters (0.78 inches). The pigmy was often used in the overflow channel.

The Argonaut is another 2-Dimensional/3-Dimensional ADV current meter. It is essentially a flowtracker without the internal data processor to compute discharge. A sonar signal is transmitted from the probe and the signal bounces back with the velocity. The user inputs a recording time and the average velocities are recorded. The processor is connected to a computer and the data is exported into a spreadsheet.

The user enters the depth and width in the spreadsheet to compute a discharge. The Argonaut was used on the overflow channel, because it could be hand held in the narrow channel.

The Global Water Flow Probe (GFP) was used to determine the velocity through the outlet pipe. The GFP is an axial flow current meter and measures velocity by counting rotations. The propeller sensor is housed inside a two inches PVC duct.

Drift tracing was also used to calculate velocities. The tracers had two purposes. It was used to calculate velocities where the instruments could not measure and as an independent check if the instruments were working properly. Five tracers were placed at each flowrate. The tracers were placed in the water before platform 1 where camera 1 was located. Camera 2 was located between platform 1 and 2 and was pointed to a grid drawn on the flume. After the tracers were recorded the video was stopped and a frame–by–frame analysis of distance and time was completed to calculate velocity.

A grid was drawn between the platforms 2 and 3. The grid was used to determine the velocity of the flow using drift tracers. The drift tracers were thrown before platform 1 and traveled through the end of the flume. Camera 1 and Camera 2 were used to find the drift tracers and collect the necessary information for the velocity. Camera 1 was used to record the initial time that the tracer entered the water. Camera 2 was used to track the distance and time traveled by the drift tracer. Each square on the grid was 1 inch by 1 inch. The grid extended from the channel to the sloped side of the banks. Figure 9 shows the grid used to track the drift tracers.

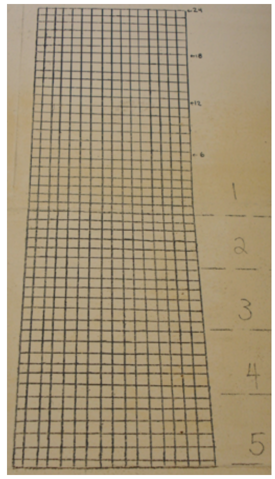

Figure 9: Grid used to collect drift tracers data.

Using camera 2 the distance and time were recorded on the datasheet. The velocity was then calculated using Equation 1 where distance was measured in inches and time in seconds. The calculated velocity was compared to the velocity data colleted by the instruments.

$$\text{Velocity} = \frac{\text{Distance}}{\text{Time}} \qquad (1)$$

The image capture speed was 30 frames per second, so that two consequent frames represent an elapsed time of 0.033 seconds or 33 milliseconds.

3.3 Data Analysis

There were 2 scenarios simulated in the trapezoidal channel. The first scenario considered the case when the channel and banks were filled with water. The flow went over the designed channel and the banks were completely submerged as shown in figure 10.

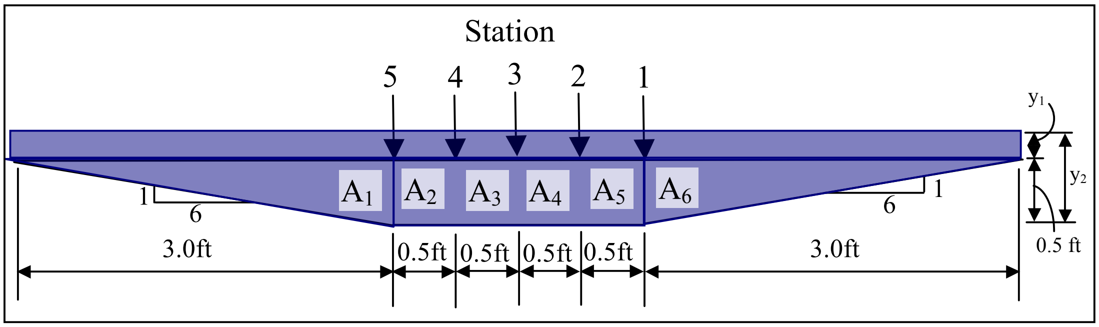

Figure 10: Trapezoidal channel with banks flooded.

When the channel and banks were filled with water the following analysis was used to create an equation to calculate the total cross-sectional flow area.

Area created by the side slopes:

$$A_1 = A_6 = \frac{1}{2}bh = \frac{1}{2}(3\text{ ft})(0.5\text{ ft}) = 0.75\text{ ft}^2$$

Area created by the rectangular channel:

$$A_2 = A_3 = A_4 = A_5 = bh = (0.5\text{ ft})(0.5\text{ ft}) = 0.25\text{ ft}^2$$

Area created after the channel and banks are full:

$$A_7 = bh = 8y_1 = 8(y_2 - 0.5) = 8y_2 - 4\text{ ft}^2$$

Total area for the flooded channel:

$$\text{Area}_t = 2(0.75\text{ ft}^2) + 4(0.25\text{ ft}^2) + 8y_2 - 4\text{ ft}^2$$

$$\text{Area}_t = 8y_2 - 1.5\text{ ft}^2$$

Where, b = the base width (feet); h = the flow depth (feet); y_1 = flow depth after the channel and banks are full (feet); y_2 = total depth of water (feet)

The second scenario observed the channel at completely full and the banks at partially full. Figure 11 shows the profile view for the channel and banks partially full.

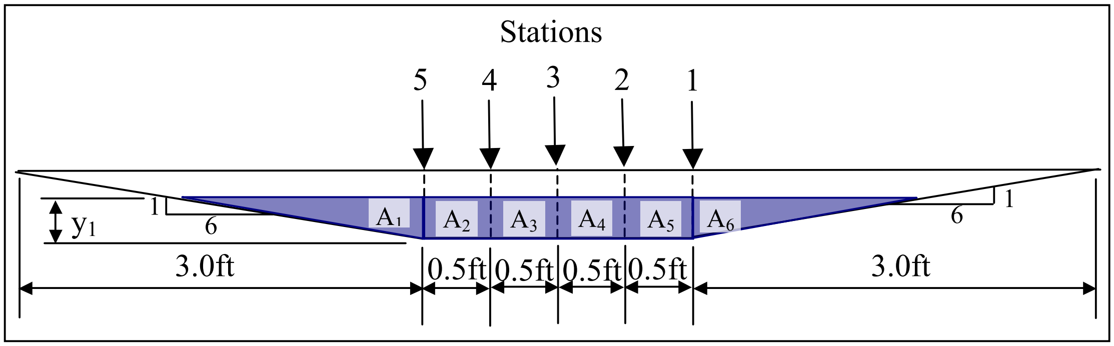

Figure 11: Channel and banks partially flooded.

Area of the triangle section:

$$A_1 = A_6 = \frac{1}{2}bh = \frac{1}{2}x_1y_1 = \frac{1}{2}(6y_1)y_1 = 3y_1^2$$

Area of the rectangular channel:

$$A_2 = A_3 = A_4 = A_6 = bh = 0.5y_1$$

Total area:

$$Area_t = 2(3y_1^2) + 4(0.5y_1)$$

$$Area_t = 6y_1^2 + 2y_1$$

Where: b = base width (feet); h = flow depth (feet); y_1 = measured flow depth (feet)

The overflow channel configuration is shown in figure 12. The overflow channel was used to aid in the mass balance of the flow. The overflow channel was 2 feet wide and was located at the end of the flume past the ditch block. The overflow channel had 3 stations and the flow depth was low. The pigmy and Argonaut were used to find velocities to calculate discharge.

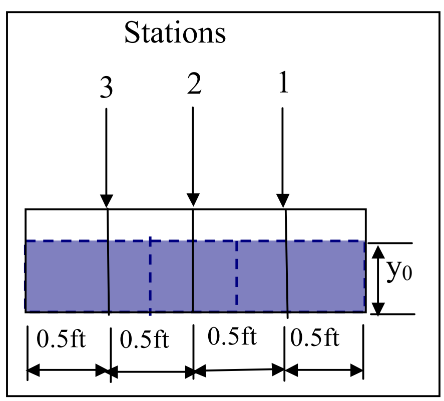

Figure 12: Overflow channel configuration.

Calculation for the areas are shown below.

Area of rectangle:

$$A_1 = A_2 = A_3 = bh = \left(\frac{2}{3}ft\right)(y_0) = \frac{2}{3}y_0$$

Total area for the overflow channel:

$$Area_t = 3\left(\frac{2}{3}y_0\right) = 2y_0$$

Where: b = base width (feet); h = flow depth (feet); y_0 = measure flow depth (feet)

Areas were calculated using the method of the mid section. The width for the area was calculated as half of the width to either side of the station. The velocity and depth were measured at each station mark. Figure 13 shows the calculations for the areas.

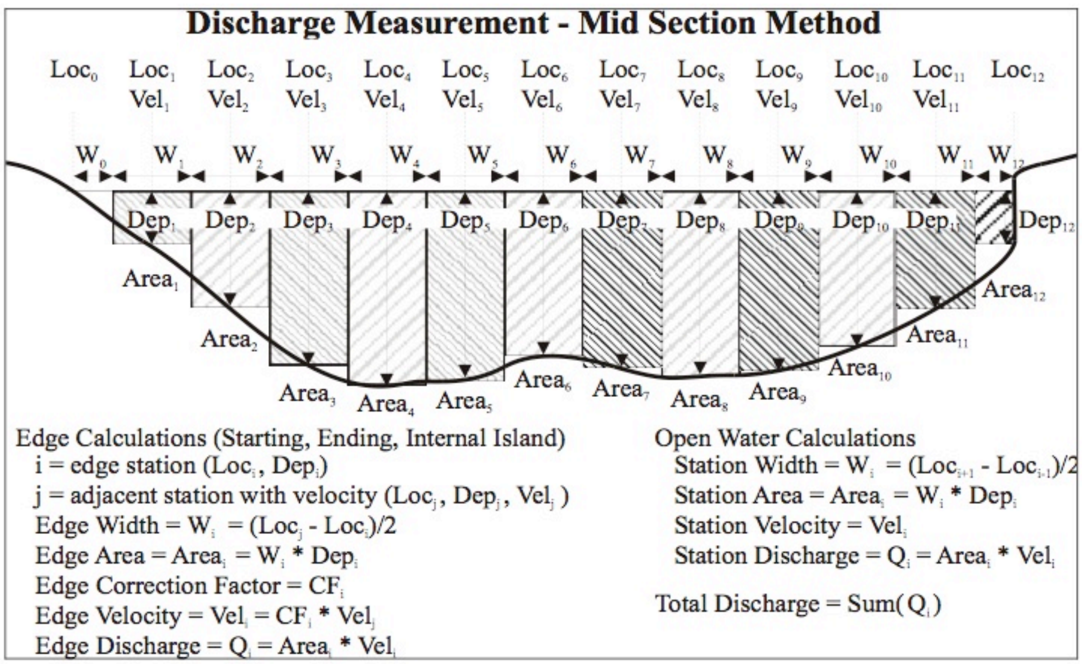

Figure 13: Mid Section Method for discharge calculations (SonTek®/YSI Inc., 2007).

From the depth and station identification, a flow area is calculated (for that portion); then, the products of station velocity and area results in the partial flow. The total flow for the section is the sum of the partial flows.

3.4 Computer Model Presentation of Physical Model Experiments

The U.S. Environmental Protection Agency (USEPA) Storm Water Management Model (SWMM) is a program that can be used to model flow through open conduits and pipes in a system. SWMM is an integrated hydrologic–hydraulic model that simulates 5 different processes from rainfall/runoff to snow melt, groundwater, flow routing and water quality. The hydrology component generates flows at different locations from rainfall–runoff models. The hydraulic component routes the flows thru various hydraulic elements in the system (i.e. pipes, ditches, weirs, lift stations, etc.).

The program allows for ponding, can report control actions and input summary and as well as skip steady periods. A minimum slope can also entered.

The program can route flow as steady flow, kinematic wave and dynamic wave. The steady flow assumes that during each time step the flow is uniform and steady. The inflow hydrograph does not changes as it travels downstream with no delays or change in pipe shapes. The steady flow method cannot be used for complex networks, it can only be used for networks that have a single outflow node. It is only valid for preliminary analysis with long-term simulations.

The Kinematic Wave routing combines the continuity equation with the momentum principle in each conduit. Kinematic wave routing does not allow for backwater effects, entrance/exit losses, flow reversal, or pressurized flow, and it is restricted to simple networks.

The Dynamic Wave routing uses the 1-Dimensional Saint Venant flow equations. The Saint Venant equations consider local and convective acceleration, hydrostatic pressure, frictional force and gravity force (McCuen, 1941).

The steady flow and kinematic wave routing methods are not appropriate for this study. The steady flow is used for uniform and steady flow and did not properly handle backwater effects. The kinematic wave is used for fully normal flows only.

The Dynamic Wave routing method was used to model the experiments. This method allows for backwater in the system along with the other functions. It incorporates Saint Venant's flow equations and is considered theoretically accurate. The approach was to run an unsteady model until equilibrium is reached; then use the equilibrium results.

3.4.1 Creation of the Models

All models were created using the same method with differences reflecting the different inlet models, slopes, and presence/absence of a ditch block. A sketch of the conceptual models are shown in Appendix B. An arbitrary origin for the system was chosen as a starting elevation. The program does not perform without elevations. Elevations started from the downstream end of the model working towards the upstream end. Figures 14 and 15 shows the SWMM model with and without a ditch block, respectively.

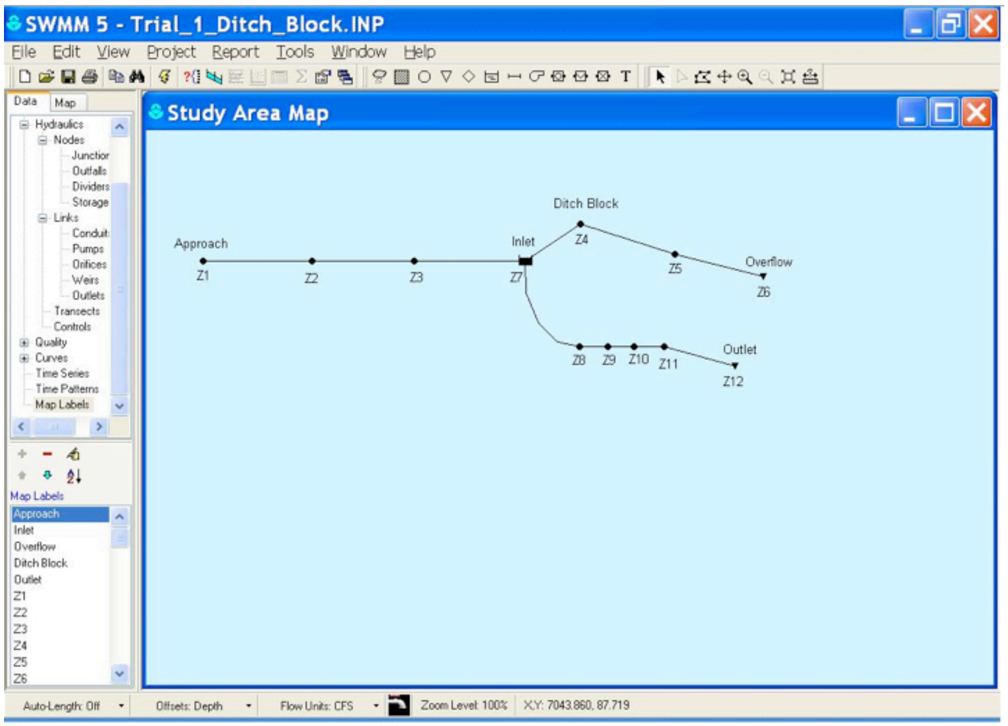

Figure 14: Configuration for the first trial set with a ditch block.

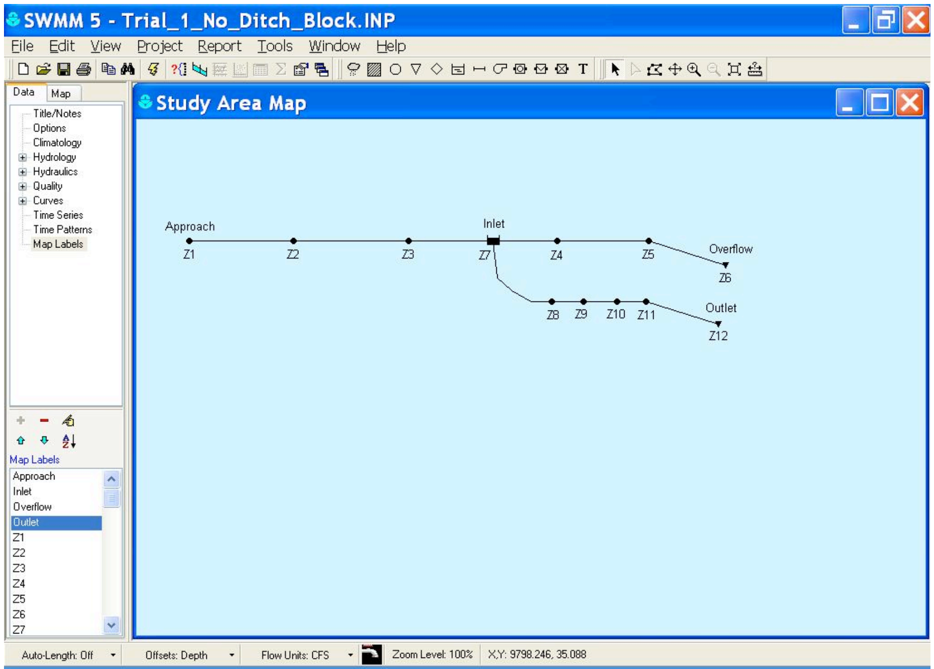

Figure 15: Configuration for the first trial set without the ditch block.

Most of the lengths for the conduits are 8 feet long for the open channel part of the system. The conduits have a trapezoidal cross-section with side slopes 6:1 (H:V). Figure 16 shows the user input for the trapezoid cross-section.

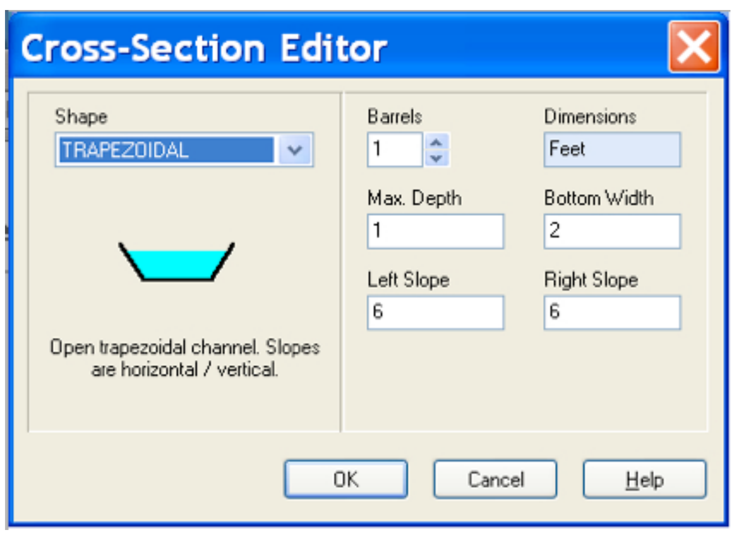

Figure 16: Trapezoid property box.

The length of the conduit coming immediately out of the box, the storage node, was set to 2 feet. For a model without the ditch block, the elevation of the conduit was set in line with the elevations of the system. For a model with a ditch block, the elevation of the conduit was raised 0.5 feet from the inline elevation.

The inlet is a node in SWMM. Exiting this node is the surface system comprised of open conduits and the subsurface system comprised of a vault box and conduits. The conduit coming out of the vault box was treated as a “special” conduit, each link was 2 feet long and the outfall conduit was 10 feet long. The special conduit had the properties to account for different elevations related to the vault box depth. The vault box contained the size of the hole for the inlet varying from 4 inches to 12 inches for different cases. Table 2 shows the invert elevations for all the slopes.

Table 2: Elevation and locations of the nodes.

		Slope 0.5%	**Slope 1.0%**	**Slope 2.0%**	
Link	**Distance (ft)**	**Inlet Elevation (ft)**	**Inlet Elevation (ft)**	**Inlet Elevation (ft)**	**Drainage System**
Z_1	8	9.68	9.85	10.19	Surface
Z_2	8	9.64	9.77	10.03	
Z_3	8	9.61	9.69	9.87	
Z_4	2	10.05	9.59	10.17	Inlet Node
Z_5	8	9.51	9.51	9.51	Surface
Z_6	8	8	8	8	
Z_7	2	8.04	8.07	8.13	Subsurface
Z_8	2	8.03	8.05	8.09	
Z_9	2	8.02	8.03	8.05	
Z_{10}	2	8.01	8.01	8.01	
Z_{11}	10	8	8	8	

There were two types of outlets used to represent the physical model. The overflow channel was modeled as a free overfall outlet, and was considered a channel for the return flow. The second type of outlet was a conduit outlet which was also modeled as a free overfall.

All roughness coefficients for the conduits were assumed to be 0.01, which represents Manning's *n* for smooth polyvinyl cloride (PVC) pipe. Figure 17 shows the input for the conduit.

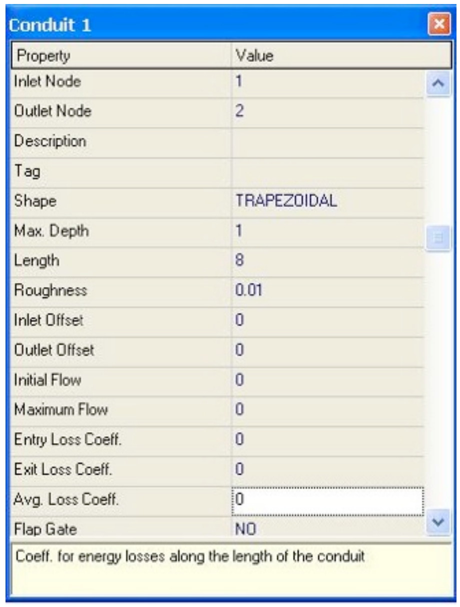

Figure 17: Sample of a conduit input box.

The following "describes" the different trials performed with SWMM.

3.4.2 Conceptual Model 1

The inlet node was treated as a storage node. The user can input the type of storage curve, the coefficient, the exponent, and the constant in the input box, figure 18.

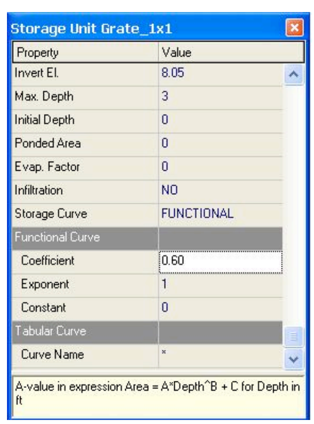

Figure 18: Storage node dialogue box.

The storage curve describes the shape of the storage unit. There are two types of storage curve, a tabular or a functional. The functional curve represents Equation 2,

$$A = A(\text{Depth})^{B} + C \qquad (2)$$

In the storage input box, A is the coefficient, B is the exponent, and C is the constant. A, B, and C represent a value for the relationship between the surface area and storage depth in Equation 2.

The tabular curve represents the area versus depth curve in a tabular manner. According to equation 2, A represents the area as well as the coefficient in the program.

The area was arbitrarily set as 60% of the actual area in an attempt to simulate hydraulics without special features[2], see table 3. For the coefficient of the storage node, the area was applied. The exponent was kept constant at 1. Table 3 shows the areas used with the different inlets.

Table 3: Areas of the Vault box and areas used in the simulations.

Inlet Type	**Area (ft^2)**	**Area in Model (ft^2)**
1' x 1' - 1	2	1.2
1' x 1' Tandem	4	2.4
2' x 2' - 1	4	2.4
2' x 4' -1	8	4.8

The special conduit had a maximum depth of the size of the inlet opening. Experiments 127–135, 241–244, 253–259 had an extra feature, a lid. The lid height (4 inches) was added to the depth of the storage node, providing extra storage for the flow.

The entrance loss coefficient was kept at a constant 0.6 and the average loss coefficient was kept at 1 on the storage node.

---

[2] This approach was eventually abandoned and the simulations were insensitive to the area specification.

3.4.3 Conceptual Model 2

For conceptual model 2, the special conduit was changed to a weir link connecting two nodes, in this case, a storage node (the inlet node) and the next node. The storage node and all the elevations for the nodes were kept the same as Trial 1 for all models. Figures 19 and 20 show the SWMM representation for the models with the ditch block and without the ditch block respectively.

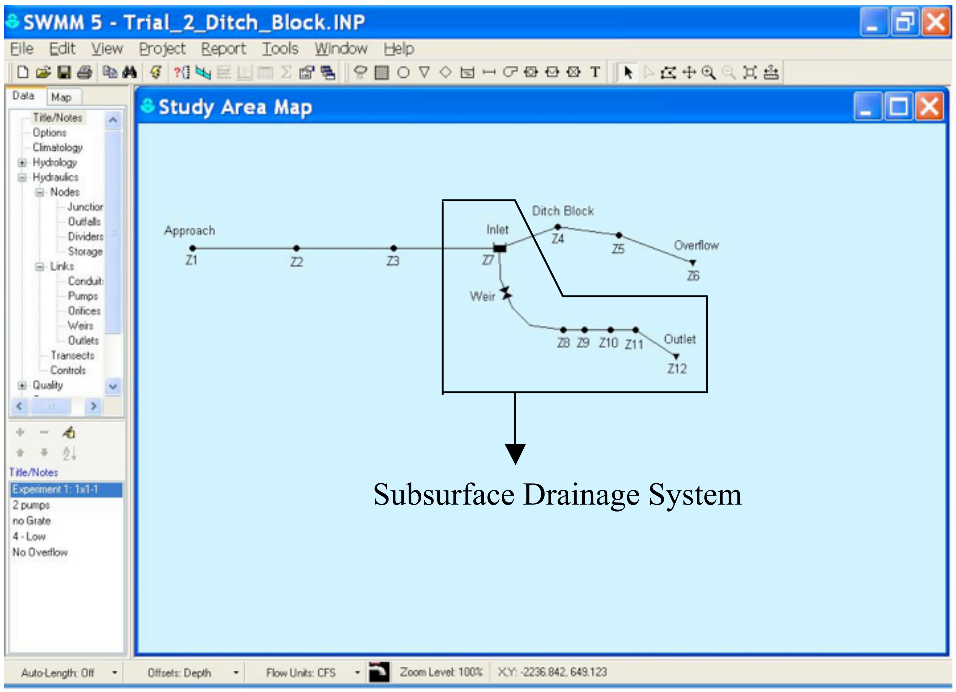

Figure 19: Weir trial with the ditch block.

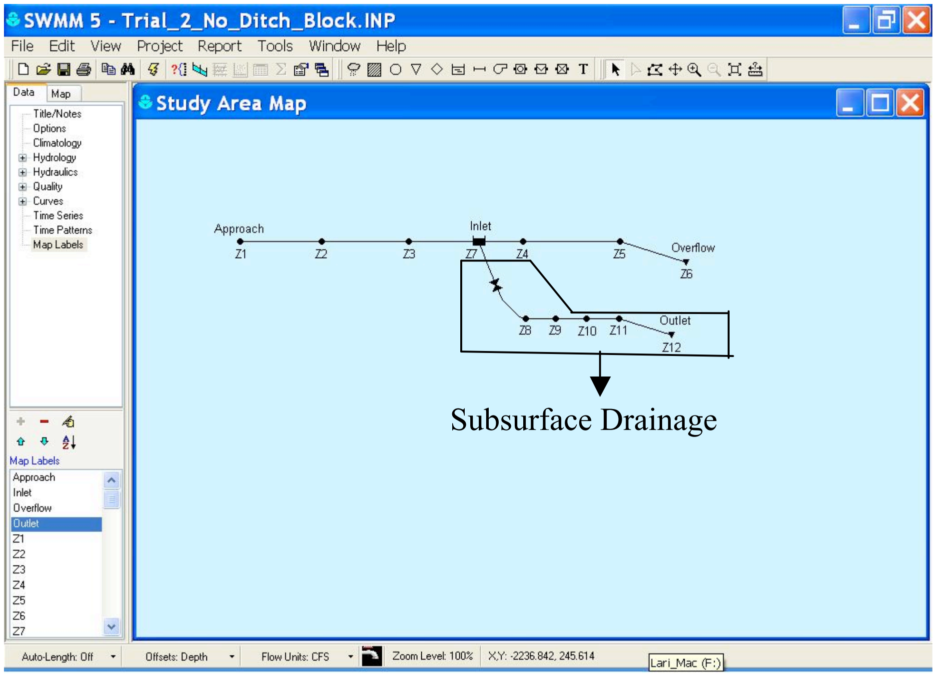

Figure 20: Weir trial without the ditch block.

The weir link required several inputs necessary for the program to operate, shown in figure 21. The property box provides information about the inlet node and outlet node. The inlet node is the storage node. Each storage node was named with the size of the vault box.

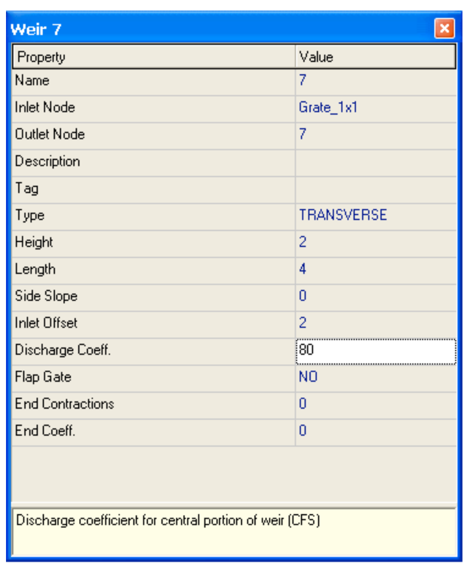

Figure 21: Special link as a weir link.

There are four types of weirs available for modeling in SWMM shown in table 4. Each type uses a different flow formula (James and others, 2005).

Table 4: Weirs available in SWMM.

Weir Type	Cross Section Shape	Flow Formula
Transverse	Rectangular	$C_wLh^{3/2}$
Side Flow	Rectangular	$C_wLh^{5/3}$
V-notch	Triangular	$C_wSh^{5/2}$
Trapezoidal	Trapezoidal	$C_wLh^{3/2}+C_{ws}Sh^{5/2}$
C_w = weir discharge coefficient, L = weir length, S = side slope of V-notch or trapezoidal weir, h = head difference across the weir, C_{ws} = discharge coefficient through sides of trapezoidal weir.		

The weir type used for the trial was the transverse type because it is structurally similar to the HEC-22 weir formula. The weir link was used as a diversion structure. The weir link controlled the amount of flow going through the subsurface drainage system. The remainder, if any, left the system through the outflow channel.

The other characteristics of interest in the dialogue box consisted of height, flap, and the discharge coefficient. The height is the height of the crest above the invert of the inlet node. A value was of 2 ft was set for the ditch block and 1.5 ft was set for the no ditch block models. The flap represents a flap gate, which allows for the control of reverse flow; in this case, it was set to no.

For the evaluation of this trial the discharge coefficient for the weir link was changed for each flow, individually, until the observed values "matched" the modeled values.

3.4.4 Conceptual Model 3

For the final conceptual model, the weir was changed from a weir link to a weir outfall. All elevations of the nodes were kept the same from previous trials. The weir outfall combined the nodes Z8 through Z11 from previous models into 1 outfall link. The weir link now directly connected to the outflow pipe. Therefore, the models have fewer nodes. The labels on the nodes were kept the same to avoid confusion between the models. Figures 22 and 23 show the SWMM configuration for the weir link as an outfall.

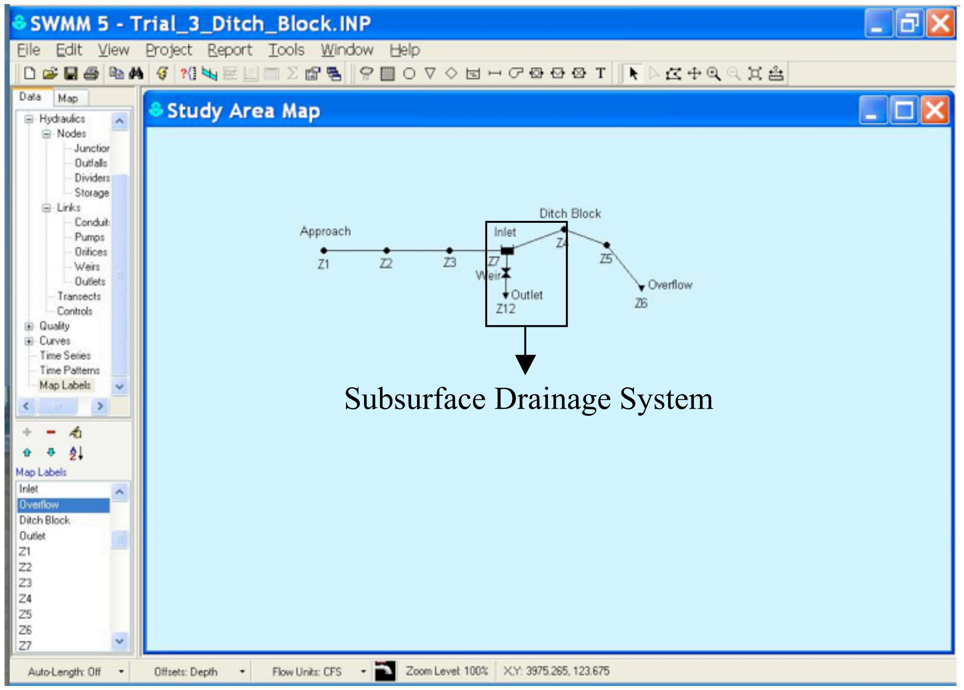

Figure 22: Weir trial with flaps, with the ditch block.

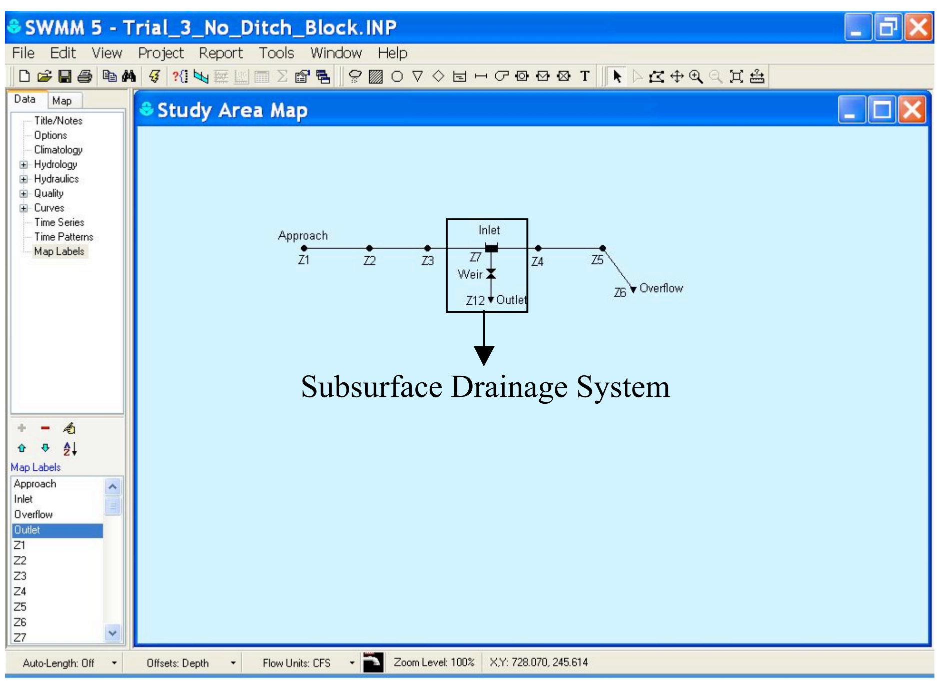

Figure 23: Weir trial with flaps, without the ditch block.

The weir link was used to control the amount of water going to the overflow channel and to the outflow pipe. The weir link is equipped with flap gates that prevent the flow from reversing back into the inlet (James et. al., 2005).

The inputs for the weir, as an outfall, are the coefficient and the exponent, shown in figure 24.

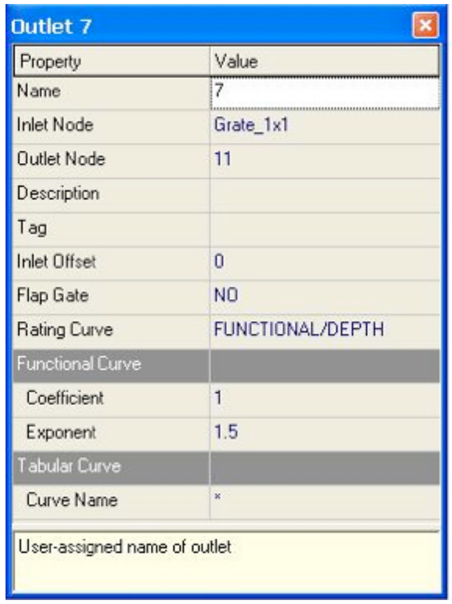

Figure 24: Weir outlet input box.

The exponent was kept at 1.5 and the coefficient was changed according to the flow. The weir outlet has 4 rating curves that can be used. The functional/depth uses a power law function ($Q=Ay^B$) to relate the depth of water above the outlet opening to the inlet node. The functional/head uses the same power function but the depth of water is calculated as a difference in head across the outlet node. The tabular/depth and tabular/head both use the same principle; but, instead, the input is a table with flow versus water depth. The exponent was kept to 1.5 to approximate the discharge equation, shown below (James et. al., 2005)

$$Q = C_w W H^{3/2} \tag{3}$$

Where: Q = discharge; C_w = weir coefficient; W = the weir width; H = head across the weir

Illustrative input and output files are included in Appendix C.

CHAPTER 4
RESULTS

Each trial was analyzed using a performance bias. These performance biases were computed for the input flow, output flow, and flow depth in the approach channel. The observed values are the values collected during the experiments and the simulated values are the values created by SWMM. The subsequent equations were used for each of the performance bias.

For the input flow: $\frac{Q_{I(obs)} - Q_{I(sim)}}{Q_{I(sim)}} \times 100\%$ (4)

For the output flow: $\frac{Q_{O(obs)} - Q_{O(sim)}}{Q_{O(sim)}} \times 100\%$ (5)

For the approach depth: $\frac{D_{A(obs)} - D_{A(sim)}}{D_{A(sim)}} \times 100\%$ (6)

The following section explains the results for each of the trials using the performance bias as a tool for comparative analyses.

4.1 Conceptual Model 1

All 274 experimental models were computed in SWMM. The simulations were complete and the overflow, outlet discharges and approach depth into the inlet node were recorded. Appendix E contains the original recorded data from the simulations. Table 5 shows the results for the performance bias.

Table 5: Conceptual Model 1 partials results.

	Slope = 0.5%									
	Observed Values				**Simulated**			**Performance Measures**		
Experiment Number	**Q_A (cfs)**	**Q_I (cfs)**	**Q_O (cfs)**	**D_A (ft)**	**Q_I (cfs)**	**Q_O (cfs)**	**D_A (ft)**	**Inlet Bias**	**Outlet Bias**	**Depth Bias**
1	0.44	0.44	0.00	0.09	0.44	0.00	0.10	-0.47	--	-11.11
2	0.63	0.46	0.17	0.34	0.63	0.00	0.23	-35.66	100.00	32.72
3	0.87	0.68	0.19	0.28	0.67	0.19	0.42	1.39	-1.97	-48.24
4	0.78	0.55	0.22	0.34	0.67	0.11	0.41	-20.79	50.95	-20.65
5	2.20	0.80	1.40	0.53	0.68	1.51	0.49	14.53	-7.62	7.12
6	0.34	0.34	0.00	0.09	0.34	0.00	0.08	-0.42	--	10.11
7	1.06	0.83	0.23	0.32	0.67	0.39	0.43	19.56	-69.27	-36.18
8	0.87	0.87	0.00	0.29	0.67	0.20	0.42	23.28	--	-44.62
9	1.68	1.18	0.49	0.36	0.68	1.00	0.47	42.60	-103.49	-30.28
10	3.11	1.49	1.63	0.44	0.69	2.42	0.51	53.56	-48.82	-14.86
						Average Bias[1] (%)		-6.9	14.3	-32

[1] Average performance bias includes all 274 that can be computed. For the complete results for trial one see appendix E.

4.2 Conceptual Model 2

The first 50 simulations were made 0.5% slope. The goal was to change the amount of flow being restricted by manipulating the coefficient on the weir link. By looking at the values of the coefficient, it was concluded that the models did not work.

In order for the experimental flows value to match the flows values in the model, the weir coefficient ranged from 4.5 to 300. The values of the coefficient were too high and the computed flows did not match the observed flow. The performance bias was calculated for all 50 simulations and table 6 shows a portion of the results. The complete results are listed in Appendix E.

Table 6: Conceptual Model 2 partial results.

	Slope = 0.5%										
	Observed Values				**Simulated Values**				**Performance Bias**		
Experiment Number	**Q_A (cfs)**	**Q_I (cfs)**	**Q_O (cfs)**	**D_A (ft)**	**Q_I (cfs)**	**Q_O (cfs)**	**D_A (ft)**	**Coefficient**	**Inlet Bias**	**Outlet Bias**	**Depth Bias**
1	0.44	0.44	0.00	0.09	0.40	0.04	0.40	80	8.66	--	-344.44
2	0.63	0.46	0.17	0.34	0.47	0.17	0.42	28	-1.21	0.00	-23.53
3	0.87	0.68	0.19	0.28	0.63	0.23	0.42	28	7.28	-21.05	-50.00
4	0.78	0.55	0.22	0.34	0.57	0.21	0.42	28	-2.76	4.55	-23.53
5	2.20	0.80	1.40	0.53	0.80	1.40	0.48	7.5	-0.55	0.00	9.43
6	0.34	0.34	0.00	0.09	0.31	0.03	0.40	80	8.44	--	-344.44
7	1.06	0.83	0.23	0.32	0.82	0.24	0.42	35	1.55	-4.35	-31.25
8	0.87	0.87	0.00	0.29	0.84	0.04	0.40	200	3.81	--	-37.93
9	1.68	1.18	0.49	0.36	1.19	0.48	0.44	28	-0.46	2.04	-22.22
10	3.11	1.49	1.63	0.44	1.46	1.65	0.49	12	1.74	-1.23	-11.36
							Average Bias[1] (%)		3.37	-0.18	-95.17

[1] Average performance bias includes all 50 simulations that can be computed. For the complete results for trial one see appendix E

4.3 Conceptual Model 3

The 274 simulations were performed with the weir as an outfall. The coefficient of the weir was modified for each of the models. The coefficients ranged from 0.10 to 1.85. Running the simulations, the modeler was able to predict a start point for the coefficients. The following trends were observed for the approach flow

1. If there was no overflow the coefficient was oberserved for the weir as 1.
2. If the flow was higher than 2.50 feet^3/second the coefficient for the weir varied from 1.1 to 1.85.
3. If the flow was lower than 1 feet^3/second the coefficient for the weir varied from 0.10 to 0.50.

These trends were observed in all three slopes used in the experiments. The coefficient varied with the flow, which increased with the increasing slope. Table 7 shows the partial results for the performance bias, the full result is located in Appendix E.

Table 7: Conceptual Model 3 partial results.

	Slope = 0.5%										
	Observed Values				**Simulated Values**				**Performance Bias**		
Experiment Number	**Q_A (cfs)**	**Q_I (cfs)**	**Q_O (cfs)**	**D_A (ft)**	**Q_I (cfs)**	**Q_O (cfs)**	**D_A (ft)**	**Coefficient**	**Inlet Bias**	**Outlet Bias**	**Depth Bias**
1	0.44	0.44	0.00	0.09	0.44	0.00	0.10	1.00	-0.47	--	-11.11
2	0.63	0.46	0.17	0.34	0.46	0.17	0.42	0.16	0.95	0.22	-22.87
3	0.87	0.68	0.19	0.28	0.69	0.17	0.42	0.24	-1.55	8.77	-48.24
4	0.78	0.55	0.22	0.34	0.55	0.23	0.42	0.19	0.84	-2.56	-23.59
5	2.20	0.80	1.40	0.53	0.81	1.38	0.48	0.27	-1.80	1.64	9.02
6	0.34	0.34	0.00	0.09	0.34	0.00	0.08	1.00	-0.42	--	10.11
7	1.06	0.83	0.23	0.32	0.81	0.25	0.42	0.28	2.75	-8.51	-33.02
8	0.87	0.87	0.00	0.29	0.87	0.00	0.14	1.00	0.38	--	51.79
9	1.68	1.18	0.49	0.36	1.17	0.50	0.44	0.40	1.23	-1.74	-21.97
10	3.11	1.49	1.63	0.44	1.52	1.60	0.49	0.50	-2.29	1.61	-10.36
							Average Bias[1] (%)		0.23	1.64	-67

[1] Average performance bias includes all 50 simulations that can be computed. For the complete results for trial one see appendix E

CHAPTER 5
CONCLUSION

Modeling real world systems in computer programs has become a challenge in the engineering field. Ideally, models would be great if predictions matched real life situations. The quality of the model is highly dependent on the modeler's understanding of the program and the system. This paper serves as a "walk-through" modeling of Type-H inlet. The trials were performed until a non-inferior solution was found.

For conceptual model 1 the simulations were performed without manipulating coefficients and the performance bias showed that the simulated inflows produced a lower outflow than the observed outflows. For conceptual model 2 the simulated inflows produced a lower outflow than the observed outflows values. Conceptual model 3 input inflows produced outflows that were 2.00% of the input inflow. Though the model highly underestimated the approach depth for all three conceptual models, conceptual model 3 is the recommended approach because it produced the least flow bias solution. It was the trial that best estimated the inlet and outlet flows and provided some useful trends to modeling inlets according to the flow.

As a general modeling guideline a Type–H inlet can be treated as a weir outfall in SWMM. The weir coefficient is assigned based on the anticipated approach flow. If the designer is trying to achieve complete capture of the flow, the simulation should be run twice; once with the $C_w = 1$ and again with $C_w = 1.85$. If both simulations suggest complete capture then the modeler is finished. If one of the simulations does not yield complete capture the modeler should increase the C_w.

Although conceptual model 3 methodology works for Type–H inlets, future research should be done to create a methodology for other types of inlet. Also, the research should include a more conclusive approach for a more precise approach depth.

REFERENCES

Argue, John R. and Pezzaniti, David (1996). How reliable are inlet (hydraulic) models at representing stormwater flow? *Science of Total Environment*, pp. 355 – 359.

Bobde, Abhijeet S. (2007). Hydraulic Performance Evaluation of Type-H Inlets. M.S. thesis, University of Houston, Houston, TX.

Brown, S., S. Stein, and J. Warner (2001). *Urban Drainage Design Manual Hydraulic Engineering Circular 22* (Second Edition; FHWA-NHI-01-021 ed.). Washington, D.C.: Federal Highway Administration.

Cassidy, J. J. (1966). Generalized hydraulic characteristics of grate inlets. *Highway Research Board Record No. 123*, 36 – 48.

Cleveland T., Rainwater K., Smirnov S., Barnes W., da Costa L., Basnet B., Aseze M., Bobde A., Mendoza Z., Singleton K., Murphy H., Ulary A. (2010). Hydraulic Capacity of Type – H Inlets. *Texas Department of Transportation*, Austin, TX.

Global Water. FP101-FP 201 Global Flow Probe User's Manual. Gold River, CA.

James, Williams, Huber, Wayne C., Rossman, Lewis E., Dickinson, Robert E., Pitt, Robert E., James, W. Robert C., Roesner, Larry A., Alrich, John A. (2005). Water Systems Models – User's guide to SWMM. CHI. Guelph, Ontario, Canada.

Larson, C. L. (1947). Investigation of flow through standard and experimental grate Inlets for street gutters. Research Report Project Report No. 3, University of Minnesota St. Anthony Falls Hydraulic Laboratory.

Larson, C. L. (1948). Experiments on flow through inlet gratings for street gutters. Research Report No. 6-B, Highway Research Board, Washington, D. C.

Li, Wen-Hsiung, Goodell, Bertram C., and Geyer, John C. (1954). Hydraulic Behavior of Storm-Water Inlets: IV. Flow into Depressed Combination Inlets. Sewage and Industrial Wastes, 26(8), pp. 967 – 975.

McCuen, Richard H. (2005). Hydrologic Analysis and Design. Pearson Prentice Hall. Upper Saddle River, NJ. pp.634

Rossman, L. (2008). Storm water management model user's manual version 5.0. Technical Report EPA/600/R-05/040, U. S. Environmental Protection Agency.

Scientific Instrument, Inc. Models 1205 & 1206: Price Type “Mini” Current Meters. Instruction and Care Manual. Milwaukee, WI.

SonTek®/YSI Inc. (2007). Flowtracker® User’s Manual: Firmware Version 3.3. SonTek®, San Diego, CA.

Thompson, J. F. WinStorm 3.05: Storm Drain Design User’s Manual. Thompson. Houston, TX.

Urbonas, Ben, 2007. Stormwater Runoff Modeling; Is it as Accurate as We Think? *Conference Urban Runoff Modeling: Intelligent Modeling to Improve Stormwater Management*, Humboldt State University, Arcata, CA. pp. 1 – 12. Correct?

APPENDIX A
INSTRUMENTATION

Acoustic Doppler Velocimeter (ADV)

The Acoustic Doppler Velocimeter (ADV) or Flowtracker was used to find discharge across the channel. The instrument has an user interface that allows for the inputs of location, depth, operators name, and file name. Figure 25 shows the ADV probe.

Figure 25: ADV Hand Held Unit (SonTek®/YSI Inc., 2007).

The probe is mounted on a two-piece, fou feet, wading rod. The wading rod has markings for every 10th of a foot. The markings on the wading rod allow the user to measure the depth of the water. On the top of the wading rod the processor can be mounted so everything is in one unit. The wading rod allows for a quick depth measure. One can lower the adv probe to the bottom of the section and the depth can be read up to the 100th.

The ADV measures current in 2D/3D. The sampling volume is cylindrical in shape located about 10.0 centimeters (4.0 inches) from the probe. Figure 26 shows the ADV probe. The probe measures a small volume of 1.02 centimeters^3 (0.062 inches^3) of a suspended particle in the water. The transmitter generates a short pulse of sound from the center of the probe and the sound bounces back to the three axis receivers.

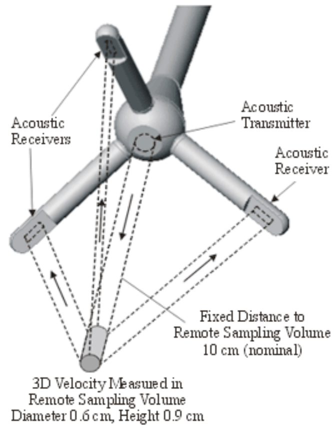

Figure 26: ADV probe sample measurement configuration (SonTek®/YSI Inc., 2007).

The sound returns to the receiver and is averaged together by the processor to produce a velocity. The instrument measures velocities as low as 0.001 meters/seconds (0.003 foot/seconds) to as high as 4.0 meters/seconds (13 feet/seconds). It measures velocities at a shallow depth of 2.0 centimeters (0.78 inch).

The user inputs the location and depth and the instrument calculates the area and discharge. Once a section is complete the instrument shows the average velocity and depth and a final discharge. The instrument has a few parameters to adjust for different water body conditions. One of the parameters is the salinity. The user can enter the salinity and the instrument will account for. The instrument can be set for both English and International System (SI) units. The user can input time from 10 to 1,000 seconds for the time the machine perform the measurements.

The instrument can calculate discharge with three different equations. The mid-section discharge equation where the velocity is taken at each location and the calculation of discharge occurs in the mid distance between each location. The mean section discharge equation the velocity is used in the location it was taken. The Japanese discharge equation the location and depth is recorded at every station but the velocity is measured at every second station.

The instrument is set up to measure velocity at different depths with different methods. Table 8 shows the methods for where velocity can be measured and how the velocity is calculated for each method.

Table 8: Velocity calculations performed by the software (SonTek®/YSI Inc., 2000).

Method	Measurement Locations	Mean Velocity Equation
0.6	0.6 * depth	$V_{mean} = V_{0.6}$
0.2/0.8 0.8/0.2	0.2 * depth 0.8 * depth	$V_{mean} = (V_{0.2} + V_{0.8}) / 2$
.2/.6/.8 .8/.6/.2	0.2 * depth 0.6 * depth 0.8 * depth	$V_{mean} = (V_{0.2} + 2*V_{0.6} + V_{0.8}) / 4$
Ice 0.6	0.6 * effective depth	$V_{mean} = 0.92*V_{0.6}$ (Correction Factor 0.92 can be changed by user)
Ice 0.5	0.5 * effective depth	$V_{mean} = 0.89*V_{0.5}$ (Correction Factor 0.89 can be changed by user)
Ice 2/8 Ice 8/2	0.2 * effective depth 0.8 * effective depth	$V_{mean} = (V_{0.2} + V_{0.8}) / 2$
Kreps 2- Kreps 2+	0.0 (near surface) 0.62 * depth	$V_{mean} = 0.31*V_{0.0} + 0.634*V_{0.62}$
5 Point+ 5 Point-	0.0 (near surface) 0.2 * depth 0.6 * depth 0.8 * depth 1.0 (near bottom)	$V_{mean} = (V_{0.0} + 3*V_{0.2} + 3*V_{0.6} + 2*V_{0.8} + V_{1.0}) / 10$
Multi Pt	Any number of points at user-specified depths	Integrated velocity average (Figure 8) Measurements can be made in any order; they are sorted by depth to calculate the integrated mean velocity. Repeat measurements at the same depth are averaged prior to calculating the integrated velocity.
None	No velocity measurement	$V_{mean} = CF * V_{adjacent}$ Mean velocity is based on the velocity from the adjacent station(s), multiplied by a user-specified correction factor. This method is used when velocity measurements cannot be made, and to specify the edges of an internal island in a multiple channel river.
Input V	User input velocity	$V_{mean} = V_{input}$ User enters an estimated velocity value. This method is used when velocity measurement is not possible, most commonly due to weed growth along a riverbank.

The process requires flowtracker software for the analysis. The software provides a spreadsheet with the file information, site details, system information, units, discharge uncertainty, and a summary. In addition it provides the measurement results for all the locations as well as the figures showing the velocity at each location and the area for the section. The file information tells the user what the file is called and the start date and time for the readings. The site details block identifies the site name and operator(s). The system information shows the sensor type the serial number, the firmware version and the software version used. The units display the units for distance, velocity, area, and discharge. The discharge uncertainty lets the user know what category –accuracy, depth, velocity, width, methods, and number of stations— had the most impact on the accuracy of the measurement. The summary block displays the averaging interval, the start edge, the man Signal to Noise Ratio (SNR), the mean temperature, the discharge equation used, the number of stations, the total width, the total area, the mean depth, mean velocity, and total discharge. Then the software produces three figures. The first figure on figure 27, shows how much each discharge at each location contributed to the overall discharge. The second figure on figure 28, shows the velocity at each location. The third figure on figure 28, displays the depth at each location.

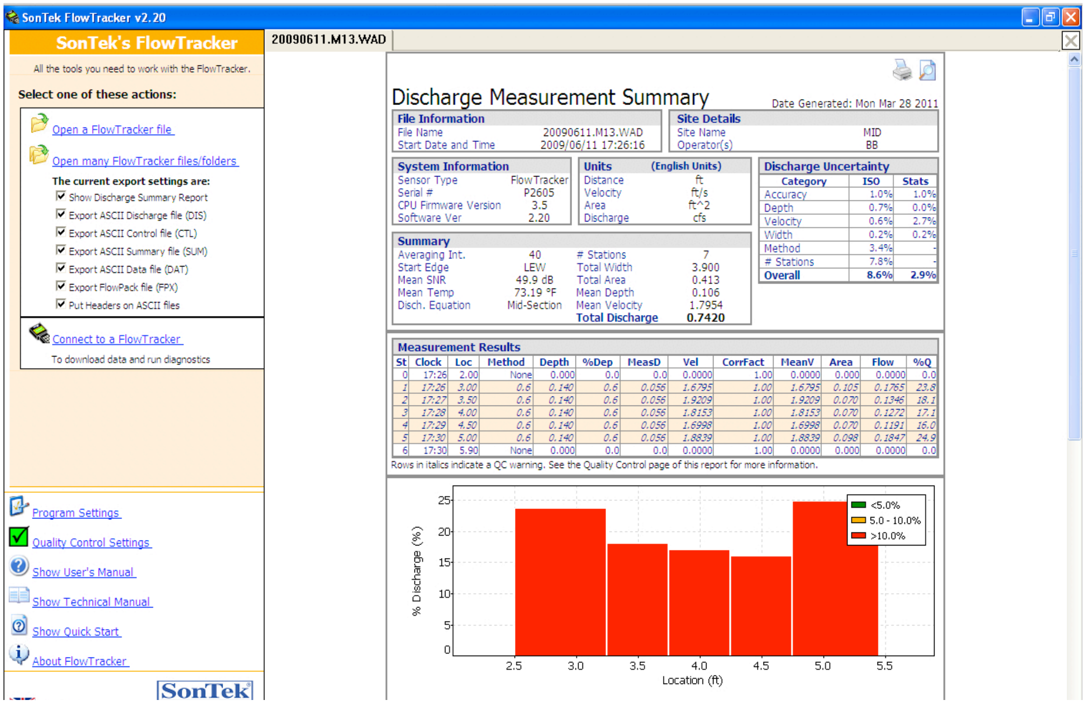

Figure 27: ADV output file (SonTek®/YSI Inc., 2000).

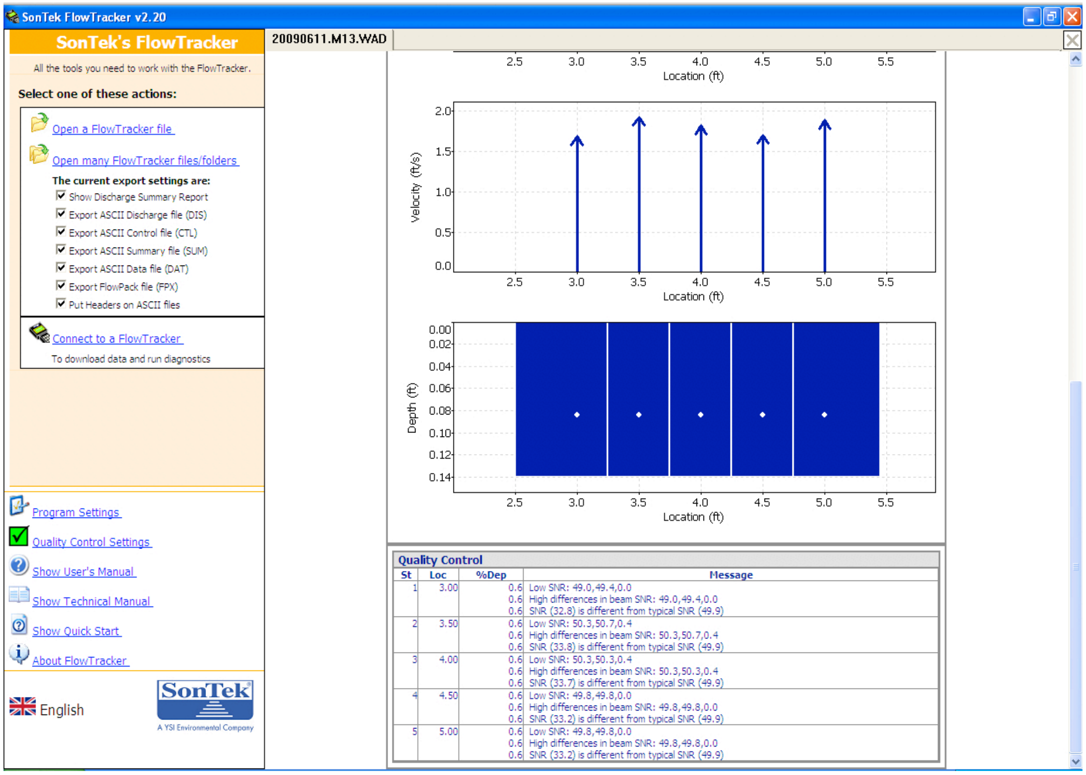

Figure 28: ADV Output file (SonTek®/YSI Inc., 2000).

Each experiment had datasheets to keep the files organized. The datasheet was used to describe the experiment set-up, the operator using the machine and the flow conditions. Figure 29 shows a representative datasheet used with the ADV.

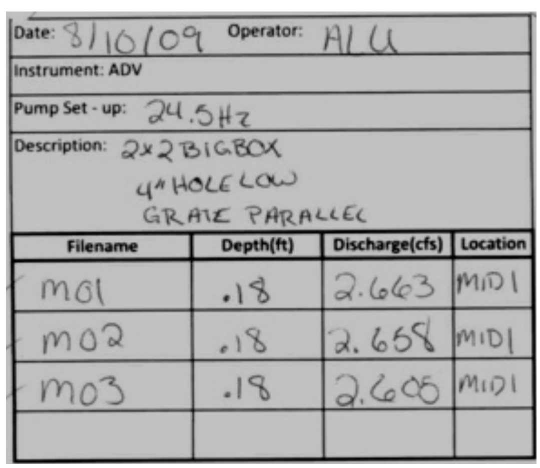

Date: 8/10/09 Operator: AL U

Instrument: ADV

Pump Set - up: 24.5Hz

Description: 2x2 BIGBOX
4" HOLE LOW
GRATE PARALLEL

Filename	Depth(ft)	Discharge(cfs)	Location
m01	.18	2.663	MID1
m02	.18	2.658	MID1
m03	.18	2.605	MID1

Figure 29: ADV datasheet.

Each platform had a specific location where the operator would seat and collect the data; table 9 shows the locations. Each platform had two sides for data collection. The side closer the upstream received 1 with their abbreviation and the other side of the platform received a 2. Platform 1 was located upstream close to the source. Platform 2 was located mid way on the flume and platform 3 was located downstream just before the inlet.

Table 9: Instrument location on the platform.

<table>
<tr><td rowspan="2">Platform 1</td><td>Up 1</td><td rowspan="2">Platform 2</td><td>Mid 1</td><td rowspan="2">Platform 3</td><td>Down 1</td></tr>
<tr><td>Up 2</td><td>Mid 2</td><td>Down 2</td></tr>
</table>

The filename was used to distinguish between the platforms. The first digit of the file name was the initial letter of the platform location, U for platform 1, M for platform 2, and D for platform 3. The following 2 digits were used for numbering the collection. Each operator ran 3 data collections for each location. The files were then sorted according to the file description and location of the data collection.

Argonaut

The Argonaut is another 2D/3D current meter. A sonar signal is transmitted from the probe and the signal bounces back with the velocity. The Argonaut works the same as the ADV. The Argonaut sampling volume is approximately 1.02 centimeters^3 (0.062 inches^3). It is located at about 10 centimeters (4 inches) from the probes. Figure 30: Argonaut.

Figure 30: 3D argonaut probe (SonTek®/YSI Inc., 2000).

Unlike the ADV, the Argonaut is not easily transported from location to location. The Argonaut is a stationary machine therefore it was only used in the overflow channel.

The Argonaut works along side of a computer. The Argonaut did not have a datasheet, all the data was directly inputted on the spreadsheet. The user sets up the recording time and the machine collects the velocity data. The data is entered in a spreadsheet along with the depth and width of the locations to create an area and discharge. The user inputs a recording time and the average velocity are recorded; see table 10.

Table 10: Spreadsheet used with the Argonaut.

Std Dev Heading	Std Dev Pitch	Std Dev Roll	Temperature (ºC)	Pressure	Std Dev Pressure	Voltage	Speed (cm/s)	Direction
0	0	0	25.16	0	0	14.2	63.34	88.3
0	0	0	25.17	0	0	14.2	44.37	87.7
0	0	0	25.16	0	0	14.2	64.13	89.1
0	0	0	25.16	0	0	14.2	87.94	91.5
0	0	0	25.17	0	0	14.2	85.36	90.6
0	0	0	25.17	0	0	14.2	71.65	89.7
0	0	0	25.17	0	0	14.2	76.17	91
0	0	0	25.17	0	0	14.2	94.36	92.2
0	0	0	25.17	0	0	14.2	93.45	91.4
0	0	0	25.17	0	0	14.2	93.1	91.2
Velocity	77.387	cm/s						
Velocity	0.7739	m/s						
Velocity	2.5383	ft/s						
Width	2.0000	ft						
Depth	0.1600	ft						
Discharge	0.8123	cfs						

Cameras

The cameras were used to track the drift tracers and record any interesting flow reactions. The cameras were set up on the side of the flume. The first camera was located upstream between platforms 1 and 2. The second camera was located between platforms 2 and 3. The third camera was suspended from the ceiling and looked down in the inlet. Figure 31 shows the camera placement.

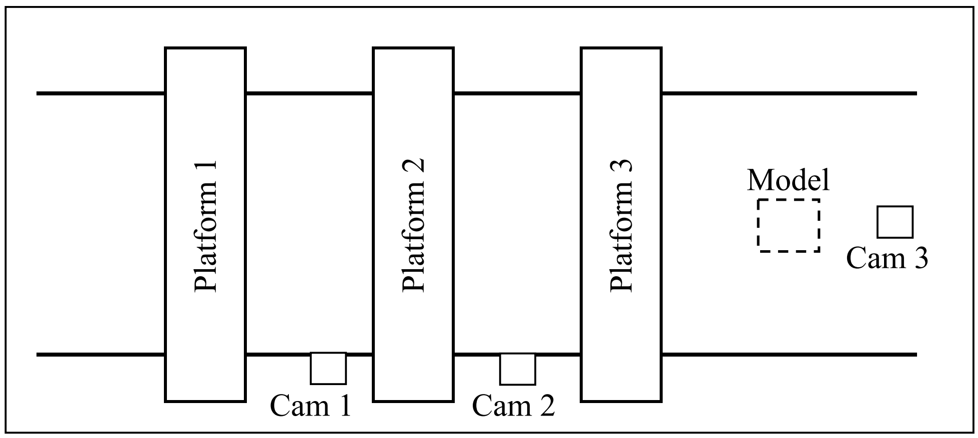

Figure 31: Cameras set-up along the flume.

The cameras 1 and 2 were used to track the drift tracers. Camera 3 was used to record the flow going through the inlet and the overflow.

Drift Tracers

The drift tracers were orange lipid-cellulose, food-grade, biodegradable, tracers. The tracers were used as tracers because it the flume surface was all white and the tracers need it to be of a good color to be able to be seen in the videos. Also, traces were a cheap tracer and the right consistency. After being used the tracers were fished out of the reservoir pool and thrown in the trash.

The drift tracers were thrown in the water after platform one and the time that was throw in was recorded. There were at least 5 drift tracers thrown during each flow. Each experiment had a set of recordings. Each experiment had two operators, the person throwing the tracers on the flow and the person recording the time that the tracers would show up on camera 2. The pump speed, flow depth and the description of the vault box were also noted in each experiment. Figure 32 shows the data sheet for the drift tracers.

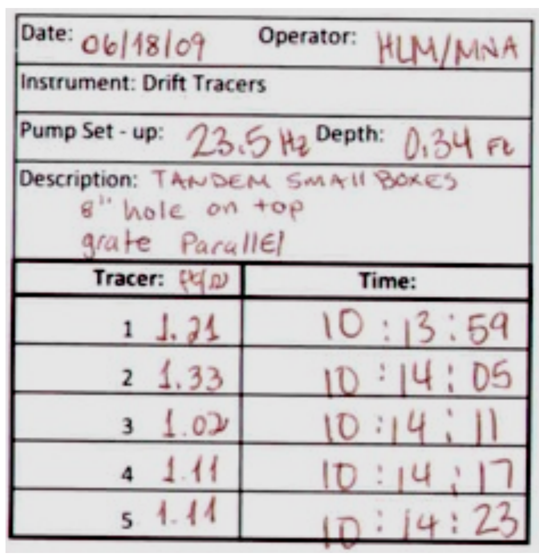

Date: 06/18/09 Operator: HLM/MNA

Instrument: Drift Tracers

Pump Set - up: 23.5 Hz Depth: 0.34 ft

Description: TANDEM SMALL BOXES
8" hole on top
grate Parallel

Tracer: [illegible]	Time:
1 1.21	10 : 13 : 59
2 1.33	10 : 14 : 05
3 1.02	10 : 14 : 11
4 1.11	10 : 14 : 17
5 1.11	10 : 14 : 23

Figure 32: Drift tracer datasheet sample.

The datasheet was used to calculate the velocity of the drift tracers. The operator would start by locating the tracer on the first camera, then finding the tracer on the second camera. The second camera had a grid drawn on the bottom of the flume to allow the operator to measure for distance. Figure 33 shows the grid located on the flume in front of camera 2.

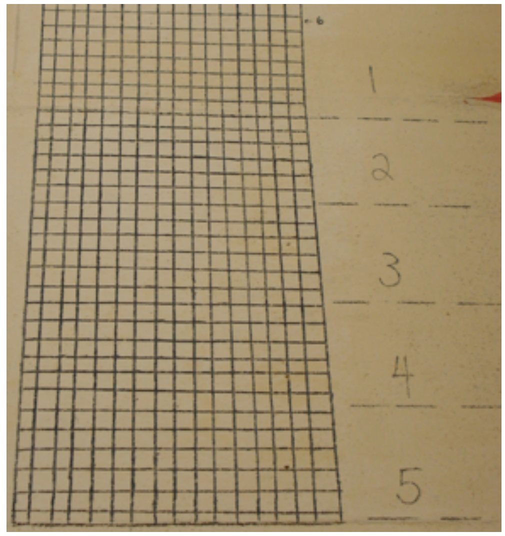

Figure 33: Tracking grid in front of camera 2.

Each square was 1 inch by 1 inch. The video software allowed the user exactly where the tracer started with the time taken at the beginning of each throw. Then the video analyst using frame-by-frame setting was able to track the tracer and determine the distance and time traveled. Using the distance and time traveled the analyst computed a velocity and the velocity was compared to the velocities being produced by the instruments. The velocity was recorded on the same datasheet of the experiment, see figure 32.

Global Flow Probe (GPF)

The GPF contains a propeller located at the bottom of the instrument. The propeller is lowered into the flow and as the propeller rotates, the software counts the number of revolutions to give velocity. Figure 34 shows the instrument. The probe handle is 3 feet to 6 feet expandable rod.

Figure 34: Global flow probe (Global Water, 2004).

The top of the expandable rod a display is connected. The display shows the velocity of the flow. The instantaneous velocity is displayed on top to the nearest 0.5 ft/s and the average velocity is displayed on the bottom. The disadvantage of the magic wand is that the user has to keep time because the machine does not have a self-counter. Each measurement was taken while holding the wand for 40 seconds. The Magic Wand was only used in the 6 in drainpipe to verify that the discharge coming into the vault box was being read correctly with the ADV. On special cases when the flow depth was high enough to cover the propeller the Magic Wand was also used on the overflow channel. Figure 35 shows the datasheet for the Wand.

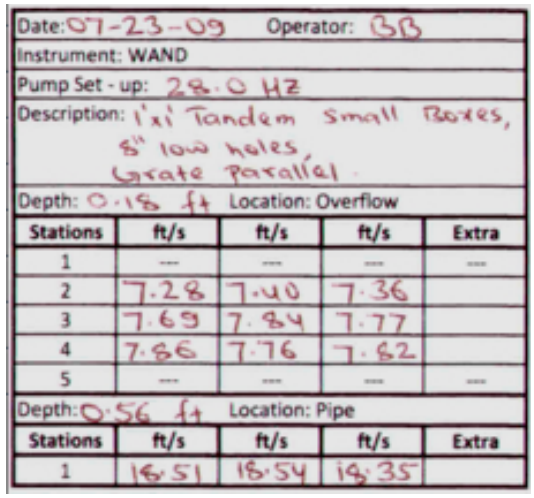

Date: 07-23-09 Operator: BB

Instrument: WAND

Pump Set - up: 28.0 HZ

Description: 1'x1' Tandem Small Boxes, 8" low holes, Grate Parallel.

Depth: 0.18 ft Location: Overflow

Stations	ft/s	ft/s	ft/s	Extra
1	---	---	---	---
2	7.28	7.40	7.36	
3	7.69	7.84	7.77	
4	7.86	7.76	7.82	
5	---	---	---	---

Depth: 0.56 ft Location: Pipe

Stations	ft/s	ft/s	ft/s	Extra
1	18.51	18.54	19.35	

Figure 2: GPF datasheet sample.

Spreadsheets were created to compute the discharge on the overflow channel and the drainpipe. The user manual provides a table located on Appendix B for the calculations for flows in partially filled pipes. (Global Flow Probe) The Appendix B was used in the spreadsheet to compute the discharge.

Table 11: Drainpipe GPF calculation spreadsheet.

Type-H Inlet Study							
Mechanical Velocity Meter Worksheet							
Date:	2009_0723	YYYY_MMDD					
Location:	Pipe						
Time:	N/A	Time of measurement					
Pump Type:	Axial	Axial or Sump					
Pump Number:	27.0 Hz	Angular frequency or number sump pumps operating					
Meter Type:	Wand	Pigmy or Wand					
Slope:	1%	Channel Longitudinal Slope					
Operator:	BB						
Description: Pipe Section							
Station is in standpipe --- THIS IS A SPECIAL WORKSHEET FOR A 1-FOOT PIPE ; DON'T USE FOR OTHER GEOMETRIES!!!!!							
Reading is meter reading							
Correction in meter correction coefficient (Pigmy = 1.00, Wand= 0.40557653)							
Measurement	Meter Type:	Depth (ft)	Reading (ft/s)	Corrected V (ft/s)	Area Factor from Table	Area (ft^2)	Q (cfs)
1	Wand	0.54	17.83	7.23	0.4526	0.4327	3.13
2	Wand	0.54	18.06	7.32	0.4526	0.4327	3.17
3	Wand	0.54	17.72	7.19	0.4526	0.4327	3.11

Pigmy

The pigmy or “mini” current meter was used to measure velocities. The pigmy is mounted on the bottom of a wading rod and connected to a machine at the top of the rod. The pigmy cups resemble an anemometer and as its cups rotate the machine counts the number of rotations and translates into velocity. Figure 36 shows the instrument.

Figure 36: Pigmy cups (Scientific Instrument).

The pigmy was used through out the channel and the overflow portion. The pigmy flow velocity measurement ranges from 0.25 feet/second to 3 feet/second (Pigmy). For flows outside of the pigmy range other instruments were used.

Datasheets were used to collect the velocities at the different location. A sample of the data sheet is shown in figure 37. The datasheet contains the date of the experiment, the operator, pump set – up, the description of the inlet and vault configuration, flow depth, and location where the measurements were taken.

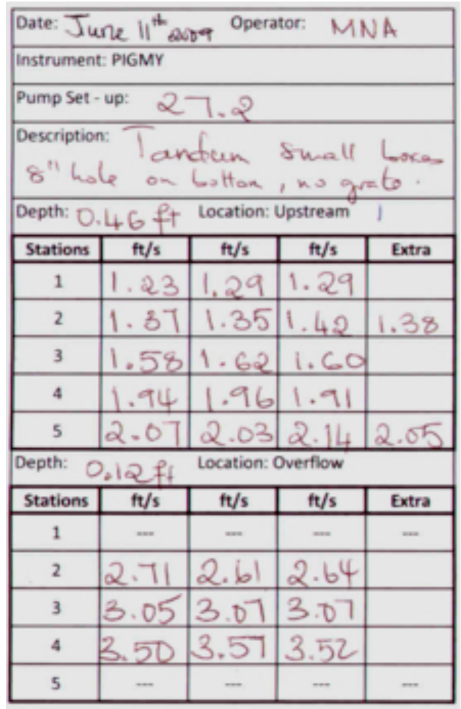

Date: June 11th 2009 Operator: MNA

Instrument: PIGMY

Pump Set - up: 27.2

Description: Tandem small boxes 8" hole on bottom, no grate.

Depth: 0.46 ft Location: Upstream

Stations	ft/s	ft/s	ft/s	Extra
1	1.23	1.29	1.29	
2	1.37	1.35	1.42	1.38
3	1.58	1.62	1.60	
4	1.94	1.96	1.91	
5	2.07	2.03	2.14	2.05

Depth: 0.12 ft Location: Overflow

Stations	ft/s	ft/s	ft/s	Extra
1	---	---	---	---
2	2.71	2.61	2.64	
3	3.05	3.07	3.07	
4	3.50	3.57	3.52	
5	---	---	---	---

Figure 37: Pygmy datasheet.

The pigmy datasheet was used to calculate discharge in the channel. Table 12 is a sample of the calculation spreadsheets used with the pigmy.

Table 12: Pigmy calculations spreadsheets.

Type-H Inlet Study						
Mechanical Velocity Meter Worksheet						
Date:	2009_0611	YYYY_MMDD				
Location:	Flume Case 1	Channel is not full of water.				
Time:		Time of measurement				
Pump Type:	Axial	Axial or Sump				
Pump Number:	4 Pumps on	Angular frequency or number sump pumps operating				
Meter Type:	Pigmy	Pigmy or Wand				
Slope:	1%	Channel Longitudinal Slope				
Operator:	KNS					
Description: Tandem small boxes, 8" hole on bottom, no grate, UP1						
Station is station from left to right looking downstream						
Station 1 and 5 are special and include triangular portion.						
Reading is meter reading						
Correction in meter correction coefficient (Pigmy = 1.00, Wand= 0.040557653)						
Station:	Meter Type:	Depth (ft)	Reading (ft/s)	Corrected V (ft/s)	Area (ft^2)	Q (cfs)
1	Pigmy	0.12	1.72	1.72	0.0588	0.101136
2	Pigmy	0.12	1.71	1.71	0.060	0.1026
3	Pigmy	0.12	1.67	1.67	0.060	0.1002
4	Pigmy	0.12	1.53	1.53	0.060	0.0918
5	Pigmy	0.12	0.968	0.968	0.0588	0.0569184
Total					0.298	0.453
Station:	Meter Type:	Depth (ft)	Reading (ft/s)	Corrected V (ft/s)	Area (ft^2)	Q (cfs)
1	Pigmy	0.12	1.73	1.73	0.0588	0.101724
2	Pigmy	0.12	1.71	1.71	0.060	0.1026
3	Pigmy	0.12	1.68	1.68	0.060	0.1008
4	Pigmy	0.12	1.55	1.55	0.060	0.093
5	Pigmy	0.12	1.04	1.04	0.0588	0.061152
Total					0.298	0.459

APPENDIX B
DRAWINGS AND SWMM

Drawings were made to determine the elevations and the configuration of the models before it was built in SWMM. Figures 38, 39, and 40 show the drawings created and Figure 41 shows the SWMM representation.

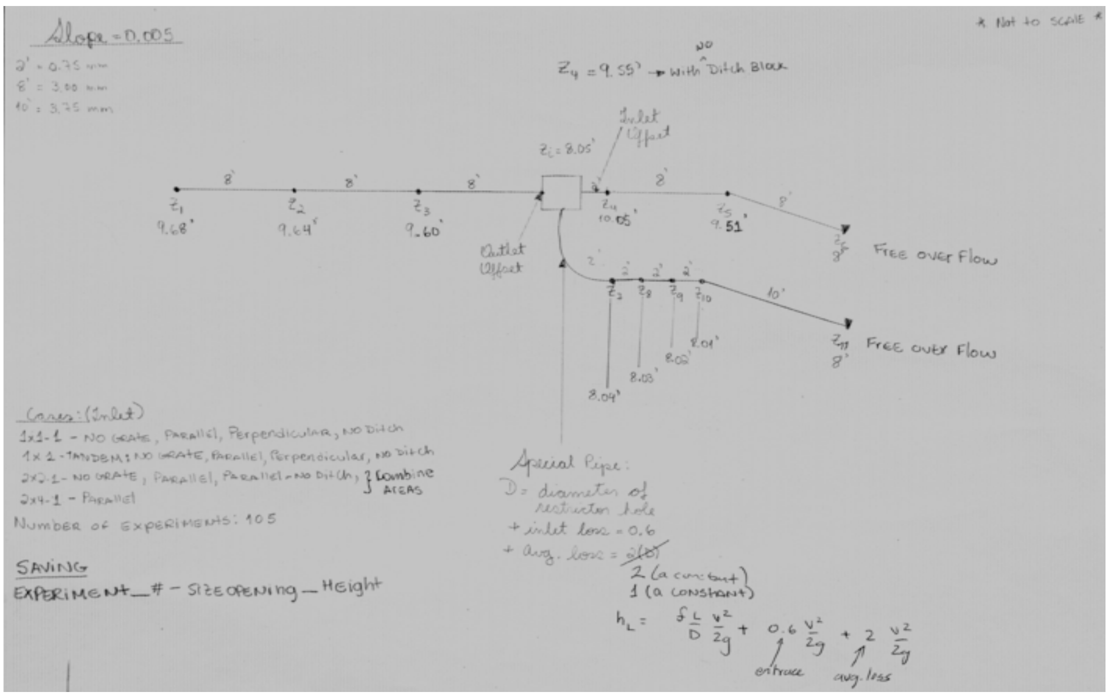

Figure 38: Drawing for slope of 0.5%.

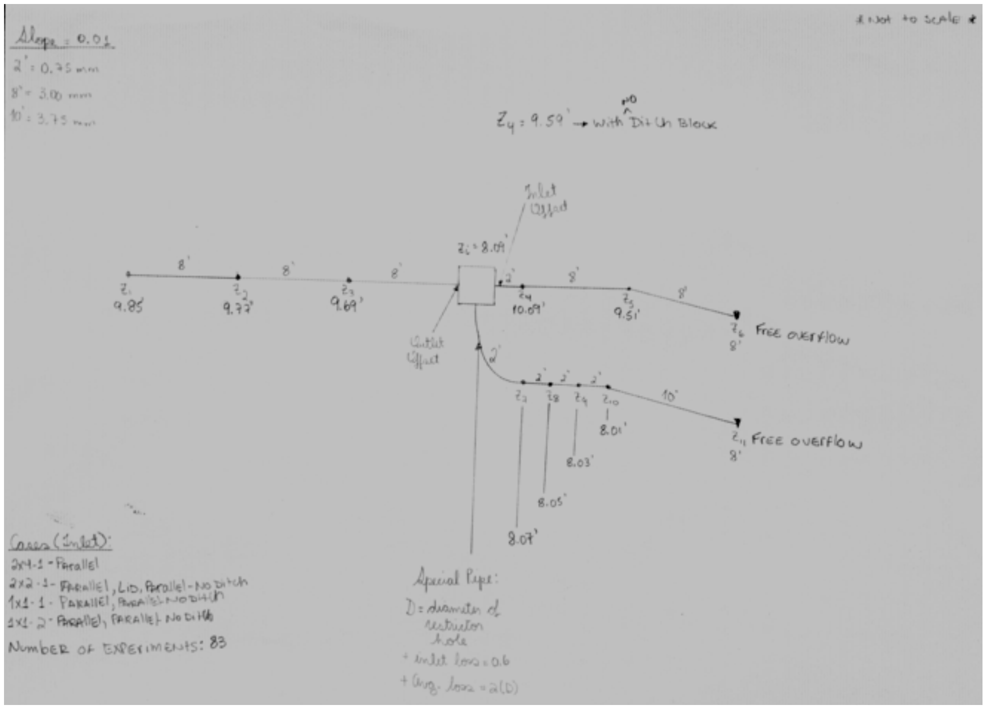

Figure 39: Drawing for slope of 1.0%.

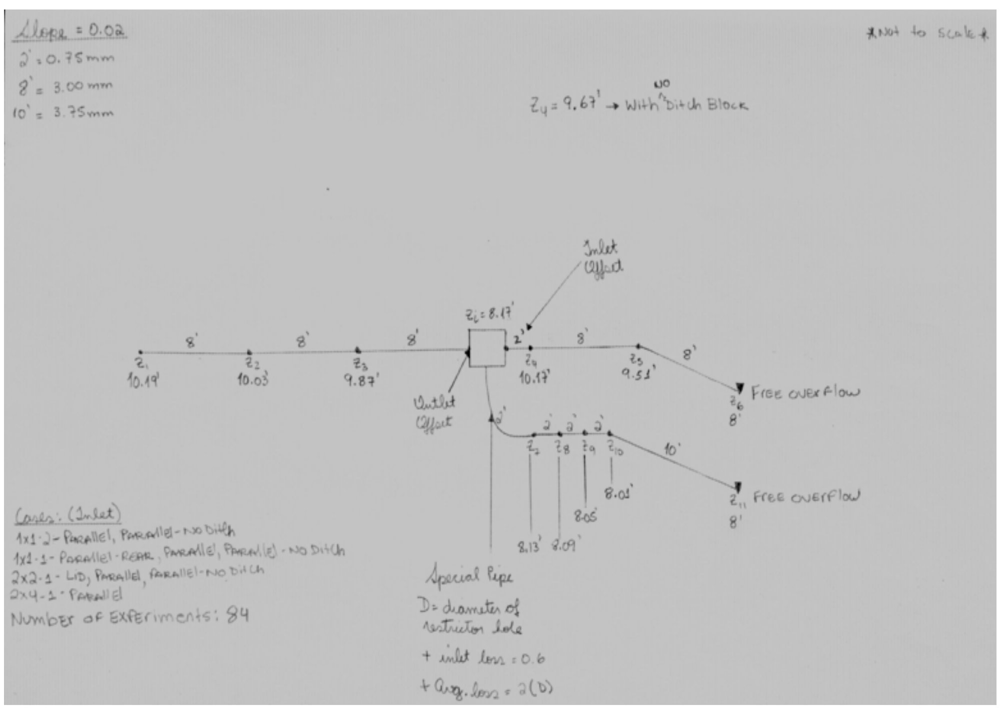

Figure 40: Drawing for slope of 2.0%.

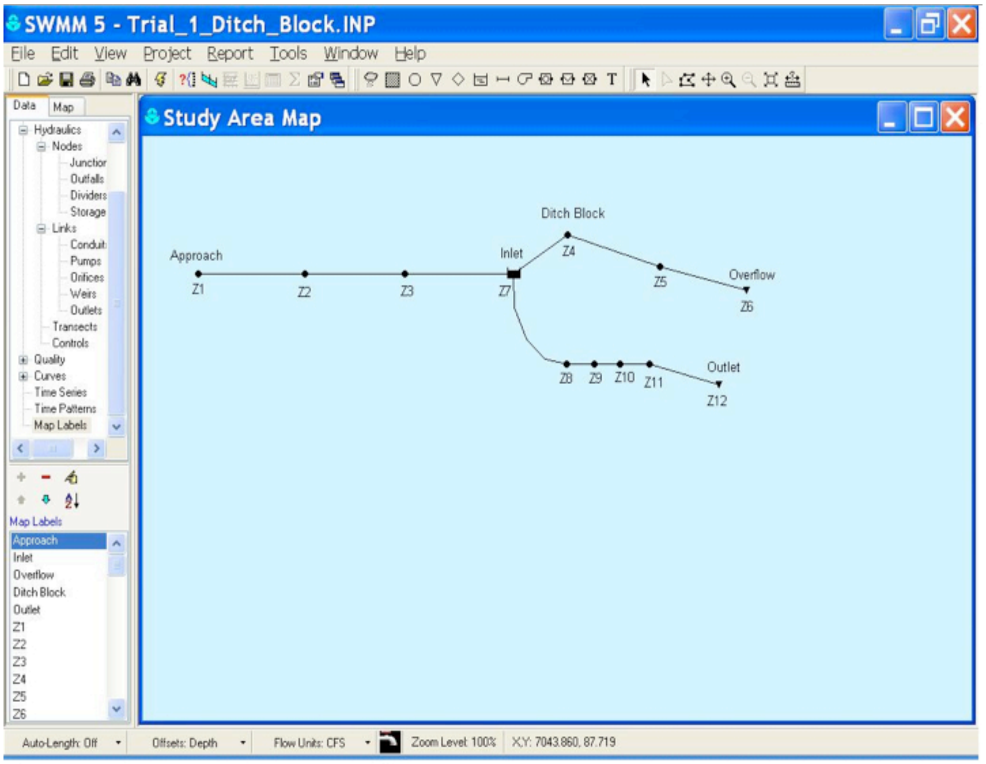

Figure 41: SWMM Representation.

APPENDIX C
SWMM INPUT FILE

Experiment 10: 1x1-1
24.5 Hz
Grate Parallel
4-Low
Overflow

```
[OPTIONS]
FLOW_UNITS          CFS
INFILTRATION        HORTON
FLOW_ROUTING        DYNWAVE
START_DATE          02/10/2010
START_TIME          00:00:00
REPORT_START_DATE   02/10/2010
REPORT_START_TIME   00:00:00
END_DATE            02/10/2010
END_TIME            06:00:00
SWEEP_START         01/01
SWEEP_END           12/31
DRY_DAYS            0
REPORT_STEP         00:00:01
WET_STEP            00:00:01
DRY_STEP            00:00:01
ROUTING_STEP        0:00:01
ALLOW_PONDING       YES
INERTIAL_DAMPING    FULL
VARIABLE_STEP       0.75
LENGTHENING_STEP    0
MIN_SURFAREA        0
NORMAL_FLOW_LIMITED BOTH
SKIP_STEADY_STATE   NO
FORCE_MAIN_EQUATION D-W
LINK_OFFSETS        DEPTH
MIN_SLOPE           0

[EVAPORATION]
;;Type       Parameters
;;---------- ----------
CONSTANT     0.0
```

```
[JUNCTIONS]
;;          Invert   Max.     Init.    Surcharge  Ponded
;;Name      Elev.    Depth    Depth    Depth      Area
;;-------------- ---------- ---------- ---------- ---------- ----------
1           9.68     1        0        0          0
2           9.64     1        0        0          0
3           9.61     1        0        0          0
4           10.05    1        0        0          0
5           9.51     1        0        0          0

[OUTFALLS]
;;          Invert   Outfall  Stage/Table    Tide
;;Name      Elev.    Type     Time Series    Gate
;;-------------- ---------- ---------- ---------------- ----
11          8        FREE                    NO
12          8        FREE                    NO

[STORAGE]
;;          Invert  Max.   Init.  Storage  Curve           Ponded
;;Name      Elev.   Depth  Depth  Curve    Params          Area
;;-------------- -------- -------- -------- ---------- -------- -------- -------- --------
Grate_1x1   8.05    3      0      FUNCTIONAL 0.60  1   0   0

[CONDUITS]
;;          Inlet       Outlet             Manning  Inlet   Outlet
;;Name      Node        Node        Length   N      Offset  Offset
;;-------------- ---------------- ---------------- ---------- ---------- ---------- ------
1           1           2           8        0.01   0       0
2           2           3           8        0.01   0       0
3           3           Grate_1x1   8        0.01   0       1.5
4           Grate_1x1   4           2        0.01   1.5     0
5           4           5           8        0.01   0       0
6           5           12          8        0.01   0       0

[OUTLETS]
;;          Inlet       Outlet      Outflow  Outlet          Qcoeff/
;;Name      Node        Node        Height   Type            QTable
;;-------------- ---------------- ---------------- ---------- --------------- ------------
7           Grate_1x1   11          0        FUNCTIONAL/DEPTH 0.50
```

APPENDIX D
SWMM OUTPUT FILE

```
EPA STORM WATER MANAGEMENT MODEL - VERSION 5.0 (Build 5.0.018)
------------------------------------------------------------

Experiment 10: 1x1-1
24.5 Hz
Grate Parallel

*******************************************************
NOTE: The summary statistics displayed in this report are
based on results found at every computational time step,
not just on results from each reporting time step.
*******************************************************

****************
Analysis Options
****************
Flow Units ............... CFS
Process Models:
  Rainfall/Runoff ........ NO
  Snowmelt ............... NO
  Groundwater ............ NO
  Flow Routing ........... YES
  Ponding Allowed ........ YES
  Water Quality .......... NO
Flow Routing Method ...... DYNWAVE
Starting Date ............ FEB-10-2010 00:00:00
Ending Date .............. FEB-10-2010 06:00:00
Antecedent Dry Days ...... 0.0
Report Time Step ......... 00:00:01
Routing Time Step ........ 1.00 sec

*************************        Volume         Volume
Flow Routing Continuity       acre-feet       10^6 gal
*************************     ---------      ---------
Dry Weather Inflow .......        0.000          0.000
Wet Weather Inflow .......        0.000          0.000
Groundwater Inflow .......        0.000          0.000
RDII Inflow ..............        0.000          0.000
```

External Inflow	1.543	0.503
External Outflow	1.540	0.502
Internal Outflow	0.000	0.000
Storage Losses	0.000	0.000
Initial Stored Volume	0.000	0.000
Final Stored Volume	0.002	0.001
Continuity Error (%)	0.093	

****

Time-Step Critical Elements

****

Link 8 (99.66%)

****

Highest Flow Instability Indexes

****

All links are stable.

****

Routing Time Step Summary

****

Minimum Time Step : 0.50 sec
Average Time Step : 0.50 sec
Maximum Time Step : 1.00 sec
Percent in Steady State : 0.00
Average Iterations per Step : 2.00

****

Node Depth Summary

****

Node	Type	Average Depth Feet	Maximum Depth Feet	Maximum HGL Feet	Time of Max Occurrence days hr:min
1	JUNCTION	0.50	0.53	10.21	0 00:00
2	JUNCTION	0.53	0.56	10.20	0 00:00
3	JUNCTION	0.56	0.59	10.20	0 00:01
4	JUNCTION	0.12	0.14	10.19	0 00:01
5	JUNCTION	0.09	0.10	9.61	0 00:01

7	JUNCTION	0.35	0.36	8.40	0	00:00
8	JUNCTION	0.36	0.36	8.39	0	00:01
9	JUNCTION	0.36	0.36	8.38	0	00:01
10	JUNCTION	0.36	0.37	8.38	0	00:01
11	OUTFALL	0.34	0.35	8.35	0	00:01
12	OUTFALL	0.09	0.10	8.10	0	00:01
Grate_1x1	STORAGE	2.12	2.14	10.19	0	00:01

****
Node Inflow Summary
****

Node	Type	Maximum Lateral Inflow CFS	Maximum Total Inflow CFS	Time of Max Occurrence days hr:min	Lateral Inflow Volume 10^6 gal	Total Inflow Volume 10^6 gal
1	JUNCTION	3.11	3.11	0 00:00	0.503	0.503
2	JUNCTION	0.00	4.21	0 00:00	0.000	0.503
3	JUNCTION	0.00	3.78	0 00:00	0.000	0.502
4	JUNCTION	0.00	2.82	0 00:01	0.000	0.391
5	JUNCTION	0.00	2.93	0 00:01	0.000	0.391
7	JUNCTION	0.00	0.70	0 00:00	0.000	0.111
8	JUNCTION	0.00	0.77	0 00:00	0.000	0.111
9	JUNCTION	0.00	0.76	0 00:00	0.000	0.111
10	JUNCTION	0.00	0.74	0 00:01	0.000	0.111
11	OUTFALL	0.00	0.70	0 00:01	0.000	0.111
12	OUTFALL	0.00	3.02	0 00:01	0.000	0.391
Grate_1x1	STORAGE	0.00	3.94	0 00:00	0.000	0.502

****
Node Surcharge Summary
****

No nodes were surcharged.
****
Node Flooding Summary
****

No nodes were flooded.

APPENDIX E

A. RESULTS

Table 13: Conceptual Model 1 results.

	Slope = 0.5%									
	Observed Values				Simulated Values			Performance Measures		
Experiment Number	Q_A (cfs)	Q_I (cfs)	Q_O (cfs)	D_A (ft)	Q_I-Link 7 (cfs)	Q_O-Link 4 (cfs)	D_A-Link 1 (ft)	Inlet Bias	Outlet Bias	Depth Bias
1	0.44	0.44	0.00	0.09	0.44	0.00	0.10	-0.47	--	-11.11
2	0.63	0.46	0.17	0.34	0.63	0.00	0.23	-35.66	100.00	32.72
3	0.87	0.68	0.19	0.28	0.67	0.19	0.42	1.39	-1.97	-48.24
4	0.78	0.55	0.22	0.34	0.67	0.11	0.41	-20.79	50.95	-20.65
5	2.20	0.80	1.40	0.53	0.68	1.51	0.49	14.53	-7.62	7.12
6	0.34	0.34	0.00	0.09	0.34	0.00	0.08	-0.42	--	10.11
7	1.06	0.83	0.23	0.32	0.67	0.39	0.43	19.56	-69.27	-36.18
8	0.87	0.87	0.00	0.29	0.67	0.20	0.42	23.28	--	-44.62
9	1.68	1.18	0.49	0.36	0.68	1.00	0.47	42.60	-103.49	-30.28
10	3.11	1.49	1.63	0.44	0.69	2.42	0.51	53.56	-48.82	-14.86
11	2.88	1.63	1.26	0.44	0.69	2.20	0.51	57.60	-75.13	-16.00
12	0.78	0.52	0.27	0.11	0.58	0.13	0.13	-12.34	51.28	-18.54
13	2.74	1.04	1.69	0.25	0.63	1.55	0.26	39.67	8.43	-5.26
14	0.27	0.27	0.00	0.10	0.27	0.00	0.07	-0.39	--	26.57
15	0.80	0.45	0.35	0.32	0.67	0.13	0.41	-47.65	62.90	-26.47
16	0.54	0.54	0.00	0.27	0.54	0.00	0.11	-0.46	--	59.90
17	1.02	0.24	0.78	0.34	0.67	0.34	0.43	-176.93	56.45	-26.99
18	2.55	0.61	1.94	0.40	0.69	1.87	0.50	-12.27	3.54	-24.19
19	0.57	0.57	0.00	0.15	0.57	0.00	0.11	0.50	--	24.66
20	0.83	0.83	0.00	0.31	0.67	0.16	0.42	19.34	--	-35.63
21	0.52	0.52	0.00	0.28	0.52	0.00	0.11	0.08	--	60.45
22	0.96	0.46	0.51	0.33	0.67	0.29	0.43	-46.69	42.69	-28.61
23	2.70	0.68	2.03	0.42	0.69	2.01	0.50	-2.20	0.76	-18.80
24	0.87	0.87	0.00	0.14	0.87	0.00	0.14	0.16	--	1.18

Table 13: Continued

	Observed Values				Simulated Values			Performance Measures		
Experiment Number	Q_A (cfs)	Q_I (cfs)	Q_O (cfs)	D_A (ft)	Q_I-Link 7 (cfs)	Q_O-Link 4 (cfs)	D_A-Link 1 (ft)	Inlet Bias	Outlet Bias	Depth Bias
25	2.39	2.39	0.00	0.27	2.39	0.00	0.28	-0.19	--	-4.96
26	3.34	2.84	0.50	0.43	2.56	0.78	0.46	9.77	-55.18	-6.36
27	5.44	3.88	1.57	0.48	2.62	2.83	0.53	32.41	-80.45	-11.38
28	0.37	0.37	0.00	0.10	0.37	0.00	0.09	-0.13	--	7.22
29	0.95	0.95	0.00	0.13	0.95	0.00	0.15	-0.28	--	-12.44
30	1.93	1.93	0.00	0.25	1.93	0.00	0.22	0.10	--	13.14
31	3.31	2.69	0.62	0.38	2.56	0.75	0.46	5.01	-21.91	-19.54
32	5.13	3.06	2.07	0.42	2.61	2.52	0.52	14.61	-21.66	-22.50
33	0.40	0.40	0.00	0.11	0.40	0.00	0.09	-0.26	--	20.00
34	0.90	0.90	0.00	0.13	0.90	0.00	0.14	0.45	--	-6.87
35	2.12	2.12	0.00	0.28	2.12	0.00	0.23	0.09	--	16.53
36	2.43	1.79	0.64	0.36	2.43	0.00	0.31	-36.08	100.00	13.34
37	3.81	1.92	1.88	0.41	2.58	1.23	0.48	-34.07	34.63	-16.72
38	0.41	0.41	0.00	0.11	0.41	0.00	0.09	-0.59	--	20.59
39	0.81	0.81	0.00	0.12	0.81	0.00	0.14	-0.27	--	-19.57
40	1.54	1.54	0.00	0.25	1.54	0.00	0.19	-0.21	--	23.82
41	2.49	1.65	0.85	0.37	2.49	0.00	0.38	-51.10	100.00	-3.26
42	3.39	1.62	1.77	0.43	2.56	0.82	0.46	-58.26	53.65	-6.79
43	0.32	0.32	0.00	0.09	0.32	0.00	0.08	-1.10	--	11.52
44	0.54	0.54	0.00	0.10	0.54	0.00	0.11	0.39	--	-13.99
45	0.76	0.76	0.00	0.12	0.76	0.00	0.13	0.36	--	-7.07
46	1.85	1.85	0.00	0.27	1.85	0.00	0.21	0.25	--	21.88
47	1.69	1.69	0.00	0.23	1.69	0.00	0.20	0.14	--	12.88
48	2.06	1.75	0.31	0.35	2.06	0.00	0.22	-17.52	100.00	37.23
49	3.54	2.20	1.34	0.42	2.57	0.97	0.47	-16.56	27.37	-12.06
50	3.45	1.69	1.76	0.43	2.56	0.89	0.47	-51.11	49.29	-10.11
51	0.82	0.82	0.00	0.12	0.82	0.00	0.14	0.14	--	-19.09
52	1.17	1.17	0.00	0.14	1.17	0.00	0.17	0.15	--	-25.20
53	3.20	3.20	0.00	0.22	2.55	0.65	0.45	20.38	--	-100.99
54	3.98	3.70	0.28	0.32	2.58	1.40	0.49	30.29	-394.82	-54.47
55	4.69	3.84	0.85	0.38	2.60	2.04	0.81	32.25	-138.83	-115.74
56	0.75	0.75	0.00	0.11	0.75	0.00	0.13	0.55	--	-18.30

Table 13: Continued

Experiment Number	Observed Values Q_A (cfs)	Q_I (cfs)	Q_O (cfs)	D_A (ft)	Simulated Values Q_I-Link 7 (cfs)	Q_O-Link 4 (cfs)	D_A-Link 1 (ft)	Performance Measures Inlet Bias	Outlet Bias	Depth Bias
57	1.23	1.23	0.00	0.15	1.23	0.00	0.17	-0.22	--	-15.73
58	3.67	3.67	0.00	0.25	2.57	1.10	0.48	30.03	--	-89.31
59	3.86	3.51	0.35	0.33	2.58	1.28	0.48	26.48	-268.77	-47.69
60	4.13	3.28	0.85	0.35	2.58	1.55	0.49	21.45	-82.91	-38.42
61	4.20	3.40	0.81	0.34	2.59	1.62	0.50	23.74	-101.04	-47.64
62	0.87	0.87	0.00	0.12	0.67	0.19	0.42	22.67	--	-250.00
63	1.33	1.33	0.00	0.27	0.68	0.65	0.45	48.88	--	-67.77
64	2.17	1.57	0.59	0.34	1.48	0.68	0.48	5.95	-14.33	-39.67
65	2.83	1.70	1.13	0.39	0.69	2.15	0.51	59.47	-90.00	-32.01
66	1.47	1.08	0.39	0.15	0.61	0.99	0.19	43.30	-153.87	-29.64
67	2.09	1.20	0.90	0.17	0.67	0.97	0.23	44.01	-8.12	-33.72
68	2.80	0.52	2.29	0.45	0.69	2.12	0.51	-33.33	7.29	-13.50
69	2.17	0.70	1.48	0.40	0.68	1.49	0.48	2.34	-0.83	-18.62
70	0.64	0.64	0.00	0.27	0.64	0.00	0.26	0.27	--	4.06
71	0.82	0.58	0.24	0.32	0.67	0.15	0.42	-15.61	38.20	-32.40
72	1.35	1.35	0.00	0.14	1.35	0.00	0.18	-0.21	--	-27.26
73	2.06	2.06	0.00	0.27	2.06	0.00	0.22	0.11	--	19.02
74	2.92	1.92	0.99	0.37	2.54	0.38	0.44	-32.05	61.77	-18.81
75	3.61	2.25	1.36	0.42	2.57	1.04	0.47	-14.35	23.67	-11.82
76	3.02	1.91	1.11	0.21	2.23	0.57	0.27	-16.94	48.75	-29.67
77	2.25	1.97	0.28	0.19	2.11	0.14	0.23	-7.36	50.64	-21.84
78	2.16	2.16	0.00	0.28	2.16	0.00	0.23	0.22	--	16.97
79	3.75	2.57	1.18	0.41	2.57	1.17	0.48	-0.10	0.85	-16.04
80	1.29	1.29	0.00	0.14	1.29	0.00	0.18	0.34	--	-25.87
81	2.07	2.07	0.00	0.27	2.07	0.00	0.22	-0.13	--	18.22
82	3.36	2.35	1.01	0.38	2.56	0.80	0.46	-8.72	20.46	-22.45
83	3.70	2.51	1.18	0.39	2.57	1.12	0.48	-2.23	5.18	-21.83
84	2.29	1.85	0.44	0.18	2.11	0.18	0.24	-14.32	59.52	-30.91
85	3.34	2.41	0.93	0.22	2.26	1.35	0.29	6.39	-45.92	-29.14
86	3.77	3.77	0.00	0.25	3.77	0.00	0.30	0.11	--	-21.84
87	4.08	4.08	0.00	0.33	4.06	0.00	0.32	0.42	--	2.70
88	3.08	3.08	0.00	0.23	3.08	0.00	0.28	-0.04	--	-24.08
89	3.65	3.65	0.00	0.24	3.66	0.00	0.30	-0.41	--	-26.17

Table 13: Continued.

Experiment Number	Q_A (cfs)	Q_I (cfs)	Q_O (cfs)	D_A (ft)	Q_I-Link 7 (cfs)	Q_O-Link 4 (cfs)	D_A-Link 1 (ft)	Inlet Bias	Outlet Bias	Depth Bias
	Observed Values				Simulated Values			Performance Measures		
90	4.10	4.10	0.00	0.33	4.07	0.00	0.32	0.79	--	2.47
91	4.79	3.78	1.01	0.37	4.79	0.00	0.37	-26.78	100.00	-0.88
92	2.40	2.00	0.40	0.19	2.40	0.00	0.24	-19.85	100.00	-24.07
93	3.88	3.31	0.56	0.22	3.85	0.03	0.31	-16.27	94.68	-38.60
94	3.03	3.03	0.00	0.21	3.03	0.00	0.27	0.14	--	-30.43
95	3.90	3.90	0.00	0.25	3.91	0.00	0.31	-0.23	--	-24.27
96	5.21	4.76	0.45	0.30	5.02	0.19	0.44	-5.50	57.54	-47.45
97	5.27	4.16	1.12	0.32	5.30	0.24	0.45	-27.52	78.50	-41.39
98	1.16	1.16	0.00	0.13	1.91	0.00	0.22	-64.65	--	-64.59
99	1.91	1.91	0.00	0.25	1.91	0.00	0.22	-0.11	--	13.45
100	2.72	1.83	0.89	0.34	2.53	0.19	0.43	-38.28	78.68	-27.55
101	3.40	1.85	1.54	0.39	2.56	0.83	0.46	-38.32	46.27	-17.43
102	0.47	0.47	0.00	0.09	0.47	0.00	0.10	0.01	--	-9.25
103	0.83	0.83	0.00	0.29	0.67	0.16	0.42	19.16	--	-43.93
104	0.76	0.76	0.00	0.25	0.67	0.09	0.41	11.79	--	-65.01
105	1.59	0.62	0.97	0.38	0.68	0.91	0.46	-10.56	6.63	-21.18
Slope = 1.0%										
106	2.29	0.66	1.64	0.24	0.69	1.60	0.38	-4.95	2.17	-58.22
107	1.62	0.60	1.02	0.22	0.69	0.93	0.35	-15.52	9.14	-55.90
108	0.84	0.84	0.00	0.16	0.68	0.16	0.31	18.59	--	-90.05
109	4.08	4.08	0.00	0.21	2.61	1.47	0.39	36.02	--	-88.25
110	3.20	3.20	0.00	0.18	2.58	0.61	0.35	19.27	--	-97.37
111	2.70	2.70	0.00	0.18	2.56	0.15	0.32	5.31	--	-75.31
112	5.43	4.13	1.30	0.21	5.07	0.36	0.37	-22.78	72.39	-76.68
113	4.30	3.87	0.43	0.19	4.30	0.00	0.26	-11.12	100.00	-37.20
114	4.04	4.04	0.00	0.19	4.04	0.00	0.25	0.02	--	-33.33
115	4.98	4.16	0.82	0.22	4.98	0.00	0.34	-19.85	100.00	-53.73
116	5.05	4.64	0.41	0.22	5.00	0.05	0.35	-7.66	87.69	-57.30
117	3.66	3.66	0.00	0.18	3.66	0.00	0.24	0.11	--	-31.09
118	2.94	2.94	0.00	0.16	2.94	0.00	0.21	-0.02	--	-31.94
119	2.18	2.18	0.00	0.14	2.18	0.00	0.18	0.14	--	-29.11
120	1.93	1.93	0.00	0.14	1.93	0.00	0.17	0.21	--	-22.01

Table 13: Continued.

Experiment Number	Observed Values				Simulated Values			Performance Measures		
	Q_A (cfs)	Q_I (cfs)	Q_O (cfs)	D_A (ft)	Q_I-Link 7 (cfs)	Q_O-Link 4 (cfs)	D_A-Link 1 (ft)	Inlet Bias	Outlet Bias	Depth Bias
121	2.82	2.10	0.72	0.16	2.57	0.26	0.33	-22.33	64.07	-101.42
122	3.62	2.13	1.49	0.19	2.60	1.02	0.37	-21.83	31.49	-93.21
123	2.14	0.73	1.41	0.23	0.69	1.45	0.37	5.08	-2.79	-57.78
124	1.55	0.62	0.93	0.22	0.69	0.86	0.35	-12.01	7.85	-58.25
125	0.82	0.82	0.00	0.16	0.68	0.14	0.30	16.84	--	-89.27
126	0.33	0.33	0.00	0.07	0.33	0.00	0.06	0.82	--	10.22
127	2.31	0.80	1.52	0.25	0.63	0.26	1.2	20.84	82.87	-385.34
128	0.94	0.94	0.00	0.19	0.59	0.11	0.5	37.53	--	-160.72
129	0.65	0.65	0.00	0.14	0.58	0.09	0.07	10.67	--	51.39
130	2.61	1.88	0.74	0.19	2.2	0.19	0.34	-17.22	74.18	-83.62
131	2.31	2.31	0.00	0.17	2.15	0.18	0.21	6.97	--	-24.32
132	1.77	1.77	0.00	0.13	1.77	0.15	0	0.09	--	100.00
133	4.74	3.60	1.14	0.21	4.24	0.26	0.44	-17.84	77.25	-109.11
134	3.04	3.04	0.00	0.18	3.04	0.2	0	-0.04	--	100.00
135	2.16	2.16	0.00	0.14	2.16	0.17	0	-0.16	--	100.00
136	4.24	2.96	1.29	0.19	4.08	0.20	0.26	-37.97	84.46	-37.32
137	2.89	2.42	0.47	0.16	2.89	0.00	0.21	-19.55	100.00	-33.29
138	2.50	2.03	0.47	0.15	2.19	0.44	0.20	-8.01	5.88	-35.14
139	3.37	1.99	1.39	0.17	2.31	1.05	0.23	-16.24	24.23	-37.45
140	1.93	0.80	1.14	0.13	1.93	0.00	0.17	-142.52	100.00	-35.52
141	1.46	0.73	0.73	0.11	0.61	0.85	0.15	16.45	-15.83	-35.68
142	2.35	0.80	1.55	0.24	0.69	1.65	0.38	13.61	-6.65	-60.39
143	0.87	0.87	0.00	0.19	0.68	0.19	0.31	21.73	--	-62.45
144	1.46	1.01	0.45	0.22	0.69	0.77	0.35	31.74	-71.85	-58.97
145	0.85	0.85	0.00	0.11	0.68	0.17	0.31	19.91	--	-175.15
146	0.97	0.97	0.00	0.13	0.97	0.00	0.12	0.23	--	11.00
147	3.82	2.55	1.26	0.23	2.60	1.21	0.38	-1.77	4.08	-68.70
148	3.22	2.38	0.84	0.23	2.58	0.63	0.35	-8.36	24.64	-53.23
149	1.30	1.30	0.00	0.14	1.30	0.00	0.14	-0.23	--	0.71
150	2.26	0.90	1.36	0.24	0.69	1.56	0.38	22.97	-14.72	-60.34
151	1.72	0.70	1.02	0.24	0.69	1.04	0.36	1.69	-1.87	-50.89
152	0.29	0.29	0.00	0.18	0.29	0.00	0.06	-0.72	--	65.91

Table 13: Continued.

	Observed Values				Simulated Values			Performance Measures		
Experiment Number	**Q_A (cfs)**	**Q_I (cfs)**	**Q_O (cfs)**	**D_A (ft)**	**Q_I-Link 7 (cfs)**	**Q_O-Link 4 (cfs)**	**D_A-Link 1 (ft)**	**Inlet Bias**	**Outlet Bias**	**Depth Bias**
153	0.52	0.52	0.00	0.17	0.52	0.00	0.08	0.60	--	52.43
154	1.68	0.45	1.23	0.12	0.62	1.20	0.16	-36.64	2.33	-35.02
155	1.29	0.37	0.92	0.10	0.61	0.68	0.14	-64.86	26.34	-34.90
156	2.21	1.09	1.12	0.14	2.12	0.09	0.18	-94.38	91.94	-33.33
157	1.56	0.95	0.61	0.11	1.56	0.00	0.15	-64.59	100.00	-31.84
158	1.48	0.58	0.90	0.11	0.61	1.22	0.15	-5.65	-35.46	-33.40
159	2.20	0.49	1.70	0.14	0.63	1.12	0.19	-27.34	34.27	-39.71
160	2.84	1.55	1.28	0.23	2.57	0.27	0.33	-65.35	78.98	-46.50
161	2.25	1.48	0.78	0.24	2.25	0.00	0.18	-52.45	100.00	23.49
162	1.27	1.27	0.00	0.16	1.27	0.00	0.14	-0.10	--	14.24
163	0.85	0.85	0.00	0.10	0.85	0.00	0.11	0.58	--	-14.85
164	3.04	1.83	1.21	0.20	2.58	0.46	0.34	-40.96	61.88	-68.80
165	2.52	2.04	0.48	0.18	2.52	0.00	0.28	-23.72	100.00	-51.76
166	1.73	1.73	0.00	0.14	1.73	0.00	0.16	-0.29	--	-13.14
167	1.28	1.28	0.00	0.10	1.28	0.00	0.14	-0.31	--	-34.62
168	1.98	0.45	1.52	0.24	0.69	1.29	0.37	-52.24	15.40	-54.22
169	1.44	0.46	0.98	0.23	0.68	0.75	0.34	-47.98	23.40	-47.24
170	0.67	0.67	0.00	0.18	0.67	0.00	0.27	0.03	--	-46.39
171	0.49	0.49	0.00	0.08	0.49	0.00	0.08	0.72	--	-6.67
172	1.85	0.47	1.38	0.12	0.62	1.58	0.17	-32.70	-14.46	-38.71
173	1.48	0.44	1.05	0.11	0.61	1.23	0.15	-40.06	-17.36	-33.80
174	2.65	1.65	0.99	0.15	2.21	0.60	0.20	-33.66	39.67	-32.06
175	3.33	1.70	1.63	0.17	2.29	1.15	0.23	-34.41	29.24	-34.94
176	2.65	1.14	1.51	0.15	2.21	0.61	0.20	-93.97	59.70	-31.96
177	3.04	1.23	1.81	0.16	2.26	1.04	0.22	-84.44	42.62	-37.21
178	2.68	1.32	1.36	0.22	0.69	1.99	0.39	47.59	-46.03	-80.14
179	2.00	1.22	0.78	0.20	0.69	1.31	0.37	43.55	-68.10	-85.85
180	1.46	1.46	0.00	0.12	0.69	0.77	0.35	52.67	--	-190.86
181	1.12	1.12	0.00	0.10	0.68	0.44	0.33	39.25	--	-233.05
182	4.90	3.73	1.17	0.22	2.63	2.26	0.41	29.47	-93.71	-86.72
183	4.24	3.66	0.58	0.20	2.62	1.62	0.39	28.34	-178.86	-92.12
184	2.69	2.69	0.00	0.15	2.56	0.14	0.32	4.92	--	-110.87

Table 13: Continued.

	Observed Values				Simulated Values			Performance Measures		
Experiment Number	**Q_A (cfs)**	**Q_I (cfs)**	**Q_O (cfs)**	**D_A (ft)**	**Q_I-Link 7 (cfs)**	**Q_O-Link 4 (cfs)**	**D_A-Link 1 (ft)**	**Inlet Bias**	**Outlet Bias**	**Depth Bias**
185	2.21	2.21	0.00	0.14	2.21	0.00	0.18	-0.09	--	-25.87
186	3.53	2.42	1.11	0.17	2.32	1.49	0.23	4.31	-34.77	-33.25
187	2.93	2.06	0.87	0.16	2.25	0.76	0.21	-9.01	12.46	-31.43
188	2.44	1.46	0.98	0.14	0.63	2.35	0.20	56.85	-140.27	-40.85
189	2.90	1.28	1.62	0.16	0.64	2.53	0.22	50.03	-56.55	-40.63
Slope = 2.0%										
190	2.89	1.52	1.37	0.14	0.70	2.19	0.23	53.86	-59.85	-69.43
191	3.04	2.20	0.84	0.16	0.70	2.34	0.24	68.12	-178.57	-47.77
192	1.78	1.78	0.00	0.10	0.69	1.08	0.19	61.16	--	-95.21
193	1.09	1.09	0.00	0.10	0.69	0.40	0.15	36.47	--	-50.50
194	5.18	3.41	1.77	0.18	2.69	2.49	0.28	21.11	-40.68	-51.97
195	3.63	3.01	0.63	0.15	2.65	0.98	0.23	11.89	-55.56	-54.88
196	2.68	2.68	0.00	0.13	2.61	0.07	0.19	2.70	--	-43.67
197	1.93	1.93	0.00	0.11	1.93	0.00	0.14	0.22	--	-31.56
198	2.49	0.71	1.77	0.16	0.70	1.79	0.22	1.74	-1.13	-40.65
199	1.92	0.62	1.30	0.14	0.69	1.22	0.19	-11.13	6.15	-39.96
200	0.90	0.90	0.00	0.15	0.68	0.21	0.14	24.24	--	8.50
201	3.29	1.98	1.31	0.15	2.64	0.65	0.22	-33.15	50.38	-48.56
202	2.57	1.95	0.61	0.13	2.57	0.00	0.18	-31.64	100.00	-38.55
203	1.56	1.56	0.00	0.09	1.56	0.00	0.13	0.26	--	-37.20
204	2.45	0.71	1.74	0.15	0.70	1.75	0.21	1.74	-0.57	-36.29
205	1.90	0.60	1.29	0.14	0.69	1.21	0.19	-14.25	6.20	-39.36
206	0.65	0.65	0.00	0.16	0.65	0.00	0.08	0.16	--	48.39
207	3.19	1.71	1.49	0.16	2.64	0.56	0.22	-54.78	62.42	-36.29
208	2.53	1.98	0.55	0.14	2.53	0.00	0.17	-27.48	100.00	-25.69
209	1.60	1.60	0.00	0.10	1.60	0.00	0.13	0.07	--	-31.09
210	1.28	1.28	0.00	0.09	1.28	0.00	0.11	0.27	--	-22.22
211	3.21	1.23	1.98	0.15	2.34	0.62	0.19	-90.45	68.69	-30.73
212	2.49	1.19	1.30	0.13	2.23	0.21	0.16	-88.15	83.85	-22.76
213	3.35	0.84	2.51	0.34	0.65	3.66	0.19	22.22	-45.82	43.32
214	2.57	0.72	1.85	0.13	0.64	2.59	0.17	11.14	-40.00	-31.11
215	3.24	1.28	1.96	0.14	0.65	1.71	0.19	49.18	12.76	-34.22

Table 13: Continued.

	Observed Values				Simulated Values			Performance Measures		
Experiment Number	Q_A (cfs)	Q_I (cfs)	Q_O (cfs)	D_A (ft)	Q_I-Link 7 (cfs)	Q_O-Link 4 (cfs)	D_A-Link 1 (ft)	Inlet Bias	Outlet Bias	Depth Bias
216	2.50	1.26	1.24	0.13	0.64	1.26	0.16	49.38	-1.61	-24.68
217	3.25	1.85	1.40	0.15	2.34	0.64	0.19	-26.42	54.29	-29.25
218	2.37	1.46	0.91	0.13	2.21	0.20	0.16	-51.65	78.02	-27.89
219	3.59	1.78	1.81	0.15	2.65	0.94	0.23	-48.93	48.07	-56.02
220	3.08	2.62	0.46	0.14	2.63	0.45	0.21	-0.33	2.17	-45.33
221	1.83	1.83	0.00	0.11	1.83	0.00	0.14	-0.03	--	-29.63
222	1.40	1.40	0.00	0.10	1.40	0.00	0.12	-0.25	--	-22.66
223	2.20	0.48	1.72	0.15	0.69	1.51	0.20	-44.07	12.21	-35.90
224	1.84	0.56	1.28	0.15	0.69	1.15	0.19	-23.78	10.16	-30.88
225	0.67	0.67	0.00	0.12	0.67	0.00	0.10	0.57	--	14.53
226	2.20	0.48	1.72	0.15	0.69	1.51	0.20	-44.07	12.21	-35.90
227	1.79	0.41	1.38	0.13	0.69	1.10	0.19	-66.62	20.29	-48.83
228	0.34	0.34	0.00	0.16	0.34	0.00	0.05	-0.64	--	68.15
229	2.98	1.40	1.58	0.16	2.63	0.35	0.21	-88.08	77.85	-29.10
230	2.08	0.91	1.17	0.14	2.08	0.00	0.15	-128.46	100.00	-10.43
231	1.19	1.19	0.00	0.10	1.19	0.00	0.11	0.04	--	-11.99
232	1.46	1.46	0.00	0.10	1.46	0.00	0.12	-0.34	--	-23.82
233	3.63	1.29	2.34	0.14	2.37	0.87	0.20	-83.55	62.82	-40.85
234	2.80	1.38	1.42	0.13	2.28	0.31	0.17	-64.68	78.17	-27.50
235	3.06	1.00	2.06	0.13	0.64	1.60	0.18	36.25	22.33	-38.34
236	2.48	0.58	1.90	0.14	0.64	2.47	0.16	-10.47	-30.00	-17.17
237	3.17	0.49	2.68	0.15	0.65	1.67	0.19	-32.75	37.69	-25.37
238	2.21	0.26	1.94	0.14	0.63	1.07	0.15	-140.18	44.85	-9.85
239	3.52	1.73	1.78	0.16	2.36	0.80	0.19	-36.38	55.06	-20.68
240	2.75	1.68	1.07	0.14	2.27	0.67	0.17	-34.98	37.38	-25.20
241	3.87	2.09	1.78	0.18	2.66	1.21	0.24	-27.16	32.02	-32.86
242	3.17	1.97	1.20	0.17	2.64	0.53	0.21	-34.29	55.83	-25.75
243	2.11	2.11	0.00	0.12	2.11	0.00	0.15	0.18	--	-23.71
244	1.35	1.35	0.00	0.10	1.35	0.00	0.12	0.24	--	-21.83
245	3.59	2.11	1.48	0.15	2.65	0.94	0.23	-25.54	36.49	-55.23
246	2.96	2.06	0.91	0.14	2.63	0.34	0.21	-27.79	62.64	-52.82
247	1.97	1.97	0.00	0.11	1.97	0.00	0.14	-0.11	--	-23.35
248	2.01	2.01	0.00	0.11	2.01	0.00	0.14	-0.09	--	-22.09

Table 13: Continued.

Experiment Number	Observed Values: Q_A (cfs)	Q_I (cfs)	Q_O (cfs)	D_A (ft)	Simulated Values: Q_I-Link 7 (cfs)	Q_O-Link 4 (cfs)	D_A-Link 1 (ft)	Performance Measures: Inlet Bias	Outlet Bias	Depth Bias
249	5.20	3.80	1.40	0.18	5.16	0.04	0.25	-35.76	97.14	-39.47
250	4.96	4.04	0.92	0.20	4.96	0.00	0.24	-22.72	100.00	-18.47
251	3.57	3.57	0.00	0.15	3.57	0.00	0.20	0.10	--	-35.90
252	2.57	2.57	0.00	0.13	2.57	0.00	0.17	0.12	--	-32.90
253	5.17	3.71	1.46	0.18	5.15	0.02	0.25	-38.83	98.63	-42.31
254	4.23	3.41	0.82	0.15	4.23	0.00	0.21	-24.03	100.00	-35.63
255	2.78	2.78	0.00	0.13	2.78	0.00	0.17	0.04	--	-28.54
256	1.79	1.79	0.00	0.11	1.79	0.00	0.14	0.16	--	-29.03
257	3.37	1.25	2.12	0.17	0.70	2.67	0.25	44.06	-25.94	-45.56
258	2.27	0.84	1.43	0.15	0.69	1.57	0.21	17.54	-9.79	-40.08
259	0.52	0.52	0.00	0.13	0.52	0.00	0.07	-0.37	--	47.37
260	2.47	0.70	1.77	0.15	0.70	1.78	0.21	0.25	-0.56	-38.16
261	2.15	0.76	1.39	0.15	0.69	1.46	0.20	8.89	-5.04	-30.78
262	0.84	0.84	0.00	0.20	0.68	0.15	0.13	18.75	--	33.33
263	3.00	0.86	2.14	0.14	0.64	3.17	0.18	25.56	-48.13	-26.76
264	2.14	0.59	1.55	0.12	0.63	2.01	0.15	-7.59	-29.68	-23.29
265	3.87	1.84	2.03	0.15	2.39	1.97	0.20	-29.57	2.96	-33.63
266	3.20	1.98	1.22	0.14	2.34	0.61	0.19	-18.20	50.00	-36.69
267	5.01	3.52	1.49	0.18	4.42	0.66	0.23	-25.57	55.70	-29.21
268	4.25	3.07	1.18	0.16	2.42	1.88	0.21	21.23	-59.32	-32.08
269	6.61	5.58	1.03	0.21	5.31	1.30	0.30	4.77	-26.21	-44.69
270	3.89	3.89	0.00	0.15	3.89	0.00	0.21	0.09	--	-40.63
271	3.68	2.05	1.63	0.15	2.65	1.03	0.23	-29.10	36.81	-57.18
272	2.24	2.24	0.00	0.12	2.24	0.00	0.15	-0.10	--	-23.63
273	2.26	0.61	1.65	0.12	0.69	1.56	0.21	-13.90	5.45	-75.00
274	1.15	1.15	0.00	0.14	0.69	0.47	0.15	40.16	--	-5.63
							Average Bias	-6.87	14.27	-31.21

Table 14: Conceptual Model 2 results.

	Slope = 0.5%										
	Observed Values				**Simulated Values**				**Performance Bias**		
Experiment Number	**Q_A (cfs)**	**Q_I (cfs)**	**Q_O (cfs)**	**D_A (ft)**	**Q_I-Link 7 (cfs)**	**Q_O-Link 4 (cfs)**	**D_A-Link 1 (ft)**	**Coefficient**	**Inlet Bias**	**Outlet Bias**	**Depth Bias**
1	0.44	0.44	0.00	0.09	0.40	0.04	0.40	80	8.66	--	-344.44
2	0.63	0.46	0.17	0.34	0.47	0.17	0.42	28	-1.21	0.00	-23.53
3	0.87	0.68	0.19	0.28	0.63	0.23	0.42	28	7.28	-21.05	-50.00
4	0.78	0.55	0.22	0.34	0.57	0.21	0.42	28	-2.76	4.55	-23.53
5	2.20	0.80	1.40	0.53	0.80	1.40	0.48	8	-0.55	0.00	9.43
6	0.34	0.34	0.00	0.09	0.31	0.03	0.40	80	8.44	--	-344.44
7	1.06	0.83	0.23	0.32	0.82	0.24	0.42	35	1.55	-4.35	-31.25
8	0.87	0.87	0.00	0.29	0.84	0.04	0.40	200	3.81	--	-37.93
9	1.68	1.18	0.49	0.36	1.19	0.48	0.44	28	-0.46	2.04	-22.22
10	3.11	1.49	1.63	0.44	1.46	1.65	0.49	12	1.74	-1.23	-11.36
11	2.88	1.63	1.26	0.44	1.68	1.20	0.48	18	-3.24	4.76	-9.09
12	0.78	0.52	0.27	0.11	0.57	0.21	0.13	5	-10.40	22.22	-18.18
13	2.74	1.04	1.69	0.25	1.05	1.94	0.26	2	-0.55	-14.79	-4.00
14	0.27	0.27	0.00	0.10	0.24	0.02	0.40	80	10.76	--	-300.00
15	0.80	0.45	0.35	0.32	0.45	0.35	0.43	28	0.83	0.00	-34.38
16	0.54	0.54	0.00	0.27	0.48	0.05	0.40	80	10.70	--	-48.15
17	1.02	0.24	0.78	0.34	0.25	0.77	0.45	4	-3.33	1.28	-32.35
18	2.55	0.61	1.94	0.40	0.62	1.93	0.50	5	-0.88	0.52	-25.00
19	0.57	0.57	0.00	0.15	0.52	0.06	0.40	80	9.23	--	-166.67
20	0.83	0.83	0.00	0.31	0.80	0.03	0.40	200	3.69	--	-29.03
21	0.52	0.52	0.00	0.28	0.47	0.05	0.40	80	9.69	--	-42.86
22	0.96	0.46	0.51	0.33	0.45	0.51	0.44	10	1.48	0.00	-33.33
23	2.70	0.68	2.03	0.42	0.66	2.05	0.50	5	2.24	-0.99	-19.05
24	0.87	0.87	0.00	0.14	0.78	0.09	0.41	80	10.49	--	-192.86
25	2.39	2.39	0.00	0.27	2.32	0.07	0.41	300	2.74	--	-51.85
26	3.34	2.84	0.50	0.43	2.84	0.50	0.45	65	-0.09	0.00	-4.65
27	5.44	3.88	1.57	0.48	3.87	1.58	0.50	33	0.16	-0.64	-4.17
28	0.37	0.37	0.00	0.10	0.33	0.04	0.40	80	10.69	--	-300.00
29	0.95	0.95	0.00	0.13	0.91	0.04	0.40	200	3.94	--	-207.69
30	1.93	1.93	0.00	0.25	1.88	0.06	0.41	300	2.69	--	-64.00
31	3.31	2.69	0.62	0.38	2.68	0.63	0.45	50	0.55	-1.61	-18.42

Table 14: Continued.

	Observed Values				Simulated Values				Performance Bias		
Experiment Number	**Q_A (cfs)**	**Q_I (cfs)**	**Q_O (cfs)**	**D_A (ft)**	**Q_I-Link 7 (cfs)**	**Q_O-Link 4 (cfs)**	**D_A-Link 1 (ft)**	**Coefficient**	**Inlet Bias**	**Outlet Bias**	**Depth Bias**
32	5.13	3.06	2.07	0.42	3.00	2.12	0.51	20	1.85	-2.42	-21.43
33	0.40	0.40	0.00	0.11	0.36	0.04	0.40	80	9.76	--	-263.64
34	0.90	0.90	0.00	0.13	0.81	0.09	0.41	80	10.41	--	-215.38
35	2.12	2.12	0.00	0.28	2.06	0.06	0.41	300	2.92	--	-46.43
36	2.43	1.79	0.64	0.36	1.77	0.65	0.45	32	0.88	-1.56	-25.00
37	3.81	1.92	1.88	0.41	1.91	1.89	0.50	14	0.75	-0.53	-21.95
38	0.41	0.41	0.00	0.11	0.37	0.04	0.40	80	9.22	--	-263.64
39	0.81	0.81	0.00	0.12	0.72	0.08	0.41	80	10.88	--	-241.67
40	1.54	1.54	0.00	0.25	1.47	0.07	0.41	200	4.34	--	-64.00
41	2.49	1.65	0.85	0.37	1.68	0.82	0.46	25	-1.95	3.53	-24.32
42	3.39	1.62	1.77	0.43	1.65	1.74	0.50	13	-2.01	1.69	-16.28
43	0.32	0.32	0.00	0.09	0.29	0.03	0.40	80	8.38	--	-344.44
44	0.54	0.54	0.00	0.10	0.49	0.05	0.40	80	9.62	--	-300.00
45	0.76	0.76	0.00	0.12	0.68	0.08	0.41	80	10.85	--	-241.67
46	1.85	1.85	0.00	0.27	1.80	0.05	0.41	300	2.94	--	-51.85
47	1.69	1.69	0.00	0.23	1.64	0.05	0.41	300	3.09	--	-78.26
48	2.06	1.75	0.31	0.35	1.75	0.31	0.43	60	0.17	0.00	-22.86
49	3.54	2.20	1.34	0.42	2.26	1.28	0.48	23	-2.50	4.48	-14.29
50	3.45	1.69	1.76	0.43	1.68	1.77	0.50	13	0.83	-0.57	-16.28
								Average Bias	3.37	-0.18	-95.17

Table 15: Conceptual Model 3 results.

	Slope = 0.5%										
	Observed Values				Simulated Values				Performance Measures		
Experiment Number	Q_A (cfs)	Q_I (cfs)	Q_O (cfs)	D_A (ft)	Q_I-Link 7 (cfs)	Q_O-Link 4 (cfs)	D_A-Link 1 (ft)	Coefficient	Inlet Bias	Outlet Bias	Depth Bias
1	0.44	0.44	0.00	0.09	0.44	0.00	0.10	1.00	-0.47	--	-11.11
2	0.63	0.46	0.17	0.34	0.46	0.17	0.42	0.16	0.95	0.22	-22.87
3	0.87	0.68	0.19	0.28	0.69	0.17	0.42	0.24	-1.55	8.77	-48.24
4	0.78	0.55	0.22	0.34	0.55	0.23	0.42	0.19	0.84	-2.56	-23.59
5	2.20	0.80	1.40	0.53	0.81	1.38	0.48	0.27	-1.80	1.64	9.02
6	0.34	0.34	0.00	0.09	0.34	0.00	0.08	1.00	-0.42	--	10.11
7	1.06	0.83	0.23	0.32	0.81	0.25	0.42	0.28	2.75	-8.51	-33.02
8	0.87	0.87	0.00	0.29	0.87	0.00	0.14	1.00	0.38	--	51.79
9	1.68	1.18	0.49	0.36	1.17	0.50	0.44	0.40	1.23	-1.74	-21.97
10	3.11	1.49	1.63	0.44	1.52	1.60	0.49	0.50	-2.29	1.61	-10.36
11	2.88	1.63	1.26	0.44	1.62	1.26	0.48	0.54	0.44	-0.30	-9.17
12	0.78	0.52	0.27	0.11	0.51	0.28	0.13	0.25	1.22	-4.93	-18.54
13	2.74	1.04	1.69	0.25	1.06	1.81	0.26	0.45	-1.50	-6.93	-5.26
14	0.27	0.27	0.00	0.10	0.27	0.00	0.07	1.00	-0.39	--	26.57
15	0.80	0.45	0.35	0.32	0.44	0.37	0.43	0.15	3.04	-5.59	-32.63
16	0.54	0.54	0.00	0.27	0.54	0.00	0.11	1.00	-0.46	--	59.90
17	1.02	0.24	0.78	0.34	0.24	0.79	0.45	0.08	0.80	-1.18	-32.90
18	2.55	0.61	1.94	0.40	0.61	1.94	0.50	0.20	0.75	-0.07	-24.19
19	0.57	0.57	0.00	0.15	0.57	0.00	0.11	1.00	0.50	--	24.66
20	0.83	0.83	0.00	0.31	0.83	0.00	0.14	1.00	0.08	--	54.79
21	0.52	0.52	0.00	0.28	0.52	0.00	0.11	1.00	0.08	--	60.45
22	0.96	0.46	0.51	0.33	0.44	0.52	0.44	0.15	3.67	-2.77	-31.61
23	2.70	0.68	2.03	0.42	0.67	2.03	0.50	0.22	0.76	-0.23	-18.80
24	0.87	0.87	0.00	0.14	0.87	0.00	0.14	1.00	0.16	--	1.18
25	2.39	2.39	0.00	0.27	2.39	0.00	0.24	1.00	-0.19	--	10.03
26	3.34	2.84	0.50	0.43	2.85	0.49	0.45	0.97	-0.45	2.51	-4.05
27	5.44	3.88	1.57	0.48	3.80	1.65	0.50	1.25	1.97	-5.21	-5.08
28	0.37	0.37	0.00	0.10	0.37	0.00	0.09	1.00	-0.13	--	7.22
29	0.95	0.95	0.00	0.13	0.95	0.00	0.15	1.00	-0.28	--	-12.44
30	1.93	1.93	0.00	0.25	1.93	0.00	0.22	1.00	0.10	--	13.14
31	3.31	2.69	0.62	0.38	2.66	0.65	0.46	0.90	1.29	-5.66	-19.54

Table 15: Continued.

	Observed Values				Simulated Values				Performance Bias		
Experiment Number	Q_A (cfs)	Q_I (cfs)	Q_O (cfs)	D_A (ft)	Q_I-Link 7 (cfs)	Q_O-Link 4 (cfs)	D_A-Link 1 (ft)	Coefficient	Inlet Bias	Outlet Bias	Depth Bias
32	5.13	3.06	2.07	0.42	3.07	2.06	0.51	1.00	-0.44	0.55	-20.14
33	0.40	0.40	0.00	0.11	0.40	0.00	0.09	1.00	-0.26	--	20.00
34	0.90	0.90	0.00	0.13	0.90	0.00	0.14	1.00	0.45	--	-6.87
35	2.12	2.12	0.00	0.28	2.12	0.00	0.23	1.00	0.09	--	16.53
36	2.43	1.79	0.64	0.36	1.77	0.65	0.45	0.60	0.88	-1.66	-25.79
37	3.81	1.92	1.88	0.41	1.92	1.88	0.50	0.63	0.23	0.09	-21.58
38	0.41	0.41	0.00	0.11	0.41	0.00	0.09	1.00	-0.59	--	20.59
39	0.81	0.81	0.00	0.12	0.81	0.00	0.14	1.00	-0.27	--	-19.57
40	1.54	1.54	0.00	0.25	1.54	0.00	0.19	1.00	-0.21	--	23.82
41	2.49	1.65	0.85	0.37	1.63	0.86	0.46	0.55	1.08	-1.72	-25.00
42	3.39	1.62	1.77	0.43	1.67	1.71	0.50	0.55	-3.24	3.33	-16.08
43	0.32	0.32	0.00	0.09	0.32	0.00	0.08	1.00	-1.10	--	11.52
44	0.54	0.54	0.00	0.10	0.54	0.00	0.11	1.00	0.39	--	-13.99
45	0.76	0.76	0.00	0.12	0.76	0.00	0.13	1.00	0.36	--	-7.07
46	1.85	1.85	0.00	0.27	1.85	0.00	0.21	1.00	0.25	--	21.88
47	1.69	1.69	0.00	0.23	1.69	0.00	0.20	1.00	0.14	--	12.88
48	2.06	1.75	0.31	0.35	1.75	0.31	0.43	0.60	0.17	-1.51	-22.68
49	3.54	2.20	1.34	0.42	2.26	1.28	0.48	0.75	-2.50	4.16	-14.44
50	3.45	1.69	1.76	0.43	1.68	1.77	0.50	0.55	0.83	-0.85	-17.14
51	0.82	0.82	0.00	0.12	0.82	0.00	0.14	1.00	0.14	--	-19.09
52	1.17	1.17	0.00	0.14	1.17	0.00	0.17	1.00	0.15	--	-25.20
53	3.20	3.20	0.00	0.22	3.20	0.00	0.34	1.00	0.08	--	-51.86
54	3.98	3.70	0.28	0.32	3.76	0.22	0.44	1.30	-1.59	22.24	-38.70
55	4.69	3.84	0.85	0.38	3.86	0.83	0.47	1.30	-0.58	2.83	-25.18
56	0.75	0.75	0.00	0.11	0.75	0.00	0.13	1.00	0.55	--	-18.30
57	1.23	1.23	0.00	0.15	1.23	0.00	0.17	1.00	-0.22	--	-15.73
58	3.67	3.67	0.00	0.25	3.67	0.00	0.41	1.30	0.07	--	-61.70
59	3.86	3.51	0.35	0.33	3.50	0.36	0.44	1.20	0.27	-3.72	-35.38
60	4.13	3.28	0.85	0.35	3.27	0.86	0.47	1.10	0.44	-1.49	-32.77
61	4.20	3.40	0.81	0.34	3.41	0.79	0.54	1.15	-0.41	1.96	-59.45
62	0.87	0.87	0.00	0.12	0.87	0.00	0.14	1.00	-0.41	--	-16.67
63	1.33	1.33	0.00	0.27	1.33	0.00	0.18	1.00	0.01	--	32.89

Table 15: Continued.

	Observed Values				Simulated Values				Performance Bias		
Experiment Number	**Q_A (cfs)**	**Q_I (cfs)**	**Q_O (cfs)**	**D_A (ft)**	**Q_I-Link 7 (cfs)**	**Q_O-Link 4 (cfs)**	**D_A-Link 1 (ft)**	**Coefficient**	**Inlet Bias**	**Outlet Bias**	**Depth Bias**
64	2.17	1.57	0.59	0.34	1.62	0.55	0.45	0.55	-2.94	7.53	-30.94
65	2.83	1.70	1.13	0.39	1.65	1.18	0.48	0.55	3.09	-4.28	-24.25
66	1.47	1.08	0.39	0.15	1.04	0.47	0.19	0.50	3.32	-20.52	-29.64
67	2.09	1.20	0.90	0.17	1.21	0.84	0.19	0.55	-1.12	6.37	-10.47
68	2.80	0.52	2.29	0.45	0.55	2.25	0.51	0.18	-6.28	1.61	-13.50
69	2.17	0.70	1.48	0.40	0.76	1.42	0.48	0.25	-9.15	3.91	-18.62
70	0.64	0.64	0.00	0.27	0.64	0.00	0.12	1.00	0.27	--	55.72
71	0.82	0.58	0.24	0.32	0.58	0.24	0.42	0.20	-0.08	1.11	-32.40
72	1.35	1.35	0.00	0.14	1.35	0.00	0.18	1.00	-0.21	--	-27.26
73	2.06	2.06	0.00	0.27	2.06	0.00	0.22	1.00	0.11	--	19.02
74	2.92	1.92	0.99	0.37	1.94	0.98	0.47	0.65	-0.86	1.41	-26.91
75	3.61	2.25	1.36	0.42	2.26	1.35	0.48	0.75	-0.56	0.92	-14.20
76	3.02	1.91	1.11	0.21	1.92	1.18	0.23	0.85	-0.69	-6.10	-10.46
77	2.25	1.97	0.28	0.19	1.94	0.26	0.20	0.95	1.29	8.33	-5.94
78	2.16	2.16	0.00	0.28	2.16	0.00	0.20	1.00	0.22	--	27.80
79	3.75	2.57	1.18	0.41	2.55	1.20	0.55	0.85	0.67	-1.69	-32.96
80	1.29	1.29	0.00	0.14	1.29	0.00	0.15	1.00	0.34	--	-4.90
81	2.07	2.07	0.00	0.27	2.07	0.00	0.19	1.00	-0.13	--	29.37
82	3.36	2.35	1.01	0.38	2.39	0.97	0.47	0.80	-1.50	3.56	-25.11
83	3.70	2.51	1.18	0.39	2.55	1.15	0.55	0.85	-1.43	2.64	-39.59
84	2.29	1.85	0.44	0.18	1.87	0.39	0.20	0.90	-1.32	12.29	-9.09
85	3.34	2.41	0.93	0.22	2.43	0.96	0.24	1.10	-0.65	-3.77	-6.88
86	3.77	3.77	0.00	0.25	3.77	0.00	0.41	1.40	0.11	--	-66.52
87	4.08	4.08	0.00	0.33	4.08	0.00	0.42	1.50	-0.07	--	-27.70
88	3.08	3.08	0.00	0.23	3.08	0.00	0.46	1.10	-0.04	--	-103.84
89	3.65	3.65	0.00	0.24	3.65	0.00	0.46	1.30	-0.13	--	-93.46
90	4.10	4.10	0.00	0.33	4.10	0.00	0.43	1.50	0.06	--	-31.05
91	4.79	3.78	1.01	0.37	3.74	1.05	0.55	1.25	1.01	-3.70	-49.95
92	2.40	2.00	0.40	0.19	2.05	0.43	0.21	1.00	-2.37	-8.62	-8.56
93	3.88	3.31	0.56	0.22	3.31	0.64	0.26	1.55	0.04	-13.43	-16.24
94	3.03	3.03	0.00	0.21	3.03	0.00	0.44	1.10	0.14	--	-112.56
95	3.90	3.90	0.00	0.25	3.90	0.00	0.45	1.40	0.03	--	-80.38

Table 15: Continued.

Experiment Number	Observed Values				Simulated Values				Performance Bias		
	Q_A (cfs)	Q_I (cfs)	Q_O (cfs)	D_A (ft)	Q_I-Link 7 (cfs)	Q_O-Link 4 (cfs)	D_A-Link 1 (ft)	Coefficient	Inlet Bias	Outlet Bias	Depth Bias
96	5.21	4.76	0.45	0.30	4.70	0.51	0.52	1.60	1.22	-13.97	-74.26
97	5.27	4.16	1.12	0.32	4.19	1.08	0.55	1.40	-0.81	3.23	-72.81
98	1.16	1.16	0.00	0.13	1.16	0.00	0.14	1.00	0.00	--	-4.74
99	1.91	1.91	0.00	0.25	1.91	0.00	0.18	1.00	-0.11	--	29.19
100	2.72	1.83	0.89	0.34	1.79	0.93	0.54	0.60	2.16	-4.37	-60.17
101	3.40	1.85	1.54	0.39	1.82	1.58	0.57	0.60	1.67	-2.28	-45.51
102	0.47	0.47	0.00	0.09	0.47	0.00	0.90	1.00	0.01	--	-883.25
103	0.83	0.83	0.00	0.29	0.83	0.00	0.12	1.00	-0.14	--	58.88
104	0.76	0.76	0.00	0.25	0.76	0.00	0.11	1.00	-0.06	--	55.73
105	1.59	0.62	0.97	0.38	0.66	0.99	0.54	0.20	-7.31	-1.58	-42.26
Slope = 1.0%											
106	2.29	0.66	1.64	0.24	0.61	1.69	0.55	0.20	7.22	-3.34	-129.01
107	1.62	0.60	1.02	0.22	0.60	1.02	0.52	0.20	-0.45	0.35	-131.63
108	0.84	0.84	0.00	0.16	0.84	0.00	0.10	1.00	-0.57	--	38.69
109	4.08	4.08	0.00	0.21	4.08	0.00	0.41	1.50	-0.01	--	-97.91
110	3.20	3.20	0.00	0.18	3.20	0.00	0.38	1.20	-0.13	--	-114.29
111	2.70	2.70	0.00	0.18	2.70	0.00	0.39	1.00	0.13	--	-113.66
112	5.43	4.13	1.30	0.21	4.20	1.23	0.53	1.40	-1.71	5.65	-153.08
113	4.30	3.87	0.43	0.19	3.81	0.49	0.50	1.30	1.55	-13.52	-163.85
114	4.04	4.04	0.00	0.19	4.04	0.00	0.39	1.50	0.02	--	-108.00
115	4.98	4.16	0.82	0.22	4.15	0.82	0.52	1.40	0.13	0.11	-135.12
116	5.05	4.64	0.41	0.22	4.67	0.38	0.50	1.60	-0.55	6.47	-124.72
117	3.66	3.66	0.00	0.18	3.66	0.00	0.45	1.30	0.11	--	-145.79
118	2.94	2.94	0.00	0.16	2.94	0.00	0.38	1.10	-0.02	--	-138.74
119	2.18	2.18	0.00	0.14	2.18	0.00	0.18	1.00	0.14	--	-29.11
120	1.93	1.93	0.00	0.14	1.93	0.00	0.16	1.00	0.21	--	-14.83
121	2.82	2.10	0.72	0.16	2.07	0.75	0.51	0.70	1.47	-3.63	-211.29
122	3.62	2.13	1.49	0.19	2.12	1.51	0.54	0.70	0.66	-1.42	-181.98
123	2.14	0.73	1.41	0.23	0.75	1.38	0.54	0.25	-3.17	2.17	-130.28
124	1.55	0.62	0.93	0.22	0.60	0.95	0.52	0.20	2.60	-1.79	-135.12
125	0.82	0.82	0.00	0.16	0.82	0.00	0.10	1.00	-0.28	--	36.91

Table 15: Continued.

	Observed Values				Simulated Values				Performance Bias		
Experiment Number	Q_A (cfs)	Q_I (cfs)	Q_O (cfs)	D_A (ft)	Q_I-Link 7 (cfs)	Q_O-Link 4 (cfs)	D_A-Link 1 (ft)	Coefficient	Inlet Bias	Outlet Bias	Depth Bias
126	0.33	0.33	0.00	0.07	0.33	0.00	0.06	1.00	0.82	--	10.22
127	2.31	0.80	1.52	0.25	0.83	1.93	0.24	0.35	-4.29	-27.13	2.93
128	0.94	0.94	0.00	0.19	0.94	0.00	0.11	1.00	0.48	--	42.64
129	0.65	0.65	0.00	0.14	0.65	0.00	0.90	1.00	-0.11	--	-525.00
130	2.61	1.88	0.74	0.19	1.85	0.77	0.19	0.85	1.43	-4.62	-2.61
131	2.31	2.31	0.00	0.17	2.31	0.00	0.18	1.30	0.05	--	-6.56
132	1.77	1.77	0.00	0.13	1.77	0.00	0.15	1.00	0.09	--	-17.57
133	4.74	3.60	1.14	0.21	3.62	1.14	0.26	1.60	-0.61	0.26	-23.56
134	3.04	3.04	0.00	0.18	3.04	0.00	0.20	1.70	-0.04	--	-11.32
135	2.16	2.16	0.00	0.14	2.16	0.00	0.17	1.20	-0.16	--	-17.31
136	4.24	2.96	1.29	0.19	3.00	1.24	0.24	1.30	-1.45	3.64	-26.76
137	2.89	2.42	0.47	0.16	2.50	0.35	0.20	1.20	-3.42	26.11	-26.94
138	2.50	2.03	0.47	0.15	2.09	0.41	0.18	1.00	-3.07	12.29	-21.62
139	3.37	1.99	1.39	0.17	1.99	1.12	0.25	0.85	-0.14	19.18	-49.40
140	1.93	0.80	1.14	0.13	0.89	1.01	0.19	0.40	-11.84	11.30	-51.46
141	1.46	0.73	0.73	0.11	0.76	0.72	0.16	0.35	-4.09	1.89	-44.72
142	2.35	0.80	1.55	0.24	0.76	1.59	0.54	0.25	4.85	-2.77	-127.93
143	0.87	0.87	0.00	0.19	0.87	0.00	0.10	1.00	-0.14	--	47.60
144	1.46	1.01	0.45	0.22	1.02	0.44	0.49	0.35	-0.91	1.80	-122.56
145	0.85	0.85	0.00	0.11	0.85	0.00	0.10	1.00	-0.12	--	11.24
146	0.97	0.97	0.00	0.13	0.97	0.00	0.11	1.00	0.23	--	18.42
147	3.82	2.55	1.26	0.23	2.55	1.26	0.53	0.85	0.18	0.12	-135.29
148	3.22	2.38	0.84	0.23	2.37	0.84	0.52	0.80	0.46	-0.48	-127.65
149	1.30	1.30	0.00	0.14	1.30	0.00	0.13	1.00	-0.23	--	7.80
150	2.26	0.90	1.36	0.24	0.90	1.35	0.54	0.30	-0.48	0.73	-127.85
151	1.72	0.70	1.02	0.24	0.75	0.98	0.52	0.25	-6.86	4.01	-117.95
152	0.29	0.29	0.00	0.18	0.29	0.00	0.06	1.00	-0.72	--	65.91
153	0.52	0.52	0.00	0.17	0.52	0.00	0.08	1.00	0.60	--	52.43
154	1.68	0.45	1.23	0.12	0.46	0.96	0.22	0.20	-1.38	21.86	-85.65
155	1.29	0.37	0.92	0.10	0.33	0.77	0.18	0.15	10.81	16.59	-73.45
156	2.21	1.09	1.12	0.14	1.05	0.94	0.22	0.45	3.73	15.83	-62.96

Table 15: Continued.

Experiment Number	Observed Values				Simulated Values				Performance Bias		
	Q_A (cfs)	Q_I (cfs)	Q_O (cfs)	D_A (ft)	Q_I-Link 7 (cfs)	Q_O-Link 4 (cfs)	D_A-Link 1 (ft)	Coefficient	Inlet Bias	Outlet Bias	Depth Bias
157	1.56	0.95	0.61	0.11	0.87	0.70	0.16	0.40	8.21	-14.63	-40.63
158	1.48	0.58	0.90	0.11	0.56	1.03	0.18	0.25	3.01	-14.36	-60.08
159	2.20	0.49	1.70	0.14	0.36	2.40	0.26		27.23	-40.85	-91.18
160	2.84	1.55	1.28	0.23	1.50	1.33	0.54	0.50	3.49	-3.57	-139.73
161	2.25	1.48	0.78	0.24	1.48	0.77	0.54	0.50	-0.28	0.93	-129.54
162	1.27	1.27	0.00	0.16	1.27	0.00	0.13	1.00	-0.10	--	20.37
163	0.85	0.85	0.00	0.10	0.85	0.00	0.10	1.00	0.58	--	-4.41
164	3.04	1.83	1.21	0.20	1.80	1.24	0.53	0.60	1.66	-2.76	-163.14
165	2.52	2.04	0.48	0.18	2.05	0.47	0.50	0.70	-0.65	2.58	-171.00
166	1.73	1.73	0.00	0.14	1.73	0.00	0.15	1.00	-0.29	--	-6.07
167	1.28	1.28	0.00	0.10	1.28	0.00	0.13	1.00	-0.31	--	-25.00
168	1.98	0.45	1.52	0.24	0.45	1.52	0.54	0.15	0.71	0.31	-125.08
169	1.44	0.46	0.98	0.23	0.45	0.99	0.52	0.15	2.07	-1.11	-125.19
170	0.67	0.67	0.00	0.18	0.67	0.00	0.09	1.00	0.03	--	51.20
171	0.49	0.49	0.00	0.08	0.49	0.00	0.08	1.00	0.72	--	-6.67
172	1.85	0.47	1.38	0.12	0.47	0.99	0.23	0.20	-0.59	28.28	-87.67
173	1.48	0.44	1.05	0.11	0.45	1.48	0.18	0.20	-3.32	-41.22	-60.56
174	2.65	1.65	0.99	0.15	1.65	0.97	0.20	0.74	0.21	2.46	-32.06
175	3.33	1.70	1.63	0.17	1.67	2.06	0.26	0.70	1.98	-26.75	-52.54
176	2.65	1.14	1.51	0.15	1.14	1.06	0.24	0.50	-0.06	29.97	-58.36
177	3.04	1.23	1.81	0.16	1.21	1.48	0.27	0.50	1.25	18.34	-68.40
178	2.68	1.32	1.36	0.22	1.35	1.32	0.54	0.45	-2.55	3.13	-149.42
179	2.00	1.22	0.78	0.20	1.19	0.82	0.51	0.40	2.64	-5.22	-156.17
180	1.46	1.46	0.00	0.12	1.46	0.00	0.14	1.00	-0.14	--	-16.34
181	1.12	1.12	0.00	0.10	1.12	0.00	0.12	1.00	-0.07	--	-21.11
182	4.90	3.73	1.17	0.22	3.74	1.15	0.53	1.25	-0.29	1.43	-141.37
183	4.24	3.66	0.58	0.20	3.67	0.56	0.50	1.25	-0.38	3.60	-146.31
184	2.69	2.69	0.00	0.15	2.69	0.00	0.39	1.00	0.09	--	-157.00
185	2.21	2.21	0.00	0.14	2.21	0.00	0.19	1.00	-0.09	--	-32.87
186	3.53	2.42	1.11	0.17	2.48	1.17	0.22	1.10	-2.29	-5.83	-27.45
187	2.93	2.06	0.87	0.16	2.01	1.02	0.21	0.90	2.61	-17.49	-31.43
188	2.44	1.46	0.98	0.14	1.45	0.79	0.20	0.65	0.69	19.23	-40.85

Table 15: Continued.

	Observed Values				Simulated Values				Performance Bias		
Experiment Number	Q_A (cfs)	Q_I (cfs)	Q_O (cfs)	D_A (ft)	Q_I-Link 7 (cfs)	Q_O-Link 4 (cfs)	D_A-Link 1 (ft)	Coefficient	Inlet Bias	Outlet Bias	Depth Bias
189	2.90	1.28	1.62	0.16	1.20	1.53	0.26	0.50	6.31	5.33	-66.19
Slope = 2.0%											
190	2.89	1.52	1.37	0.14	1.50	1.39	0.48	0.50	1.13	-1.14	-253.59
191	3.04	2.20	0.84	0.16	2.22	0.84	0.46	0.75	-1.10	0.28	-183.22
192	1.78	1.78	0.00	0.10	1.78	0.00	0.13	1.00	-0.20	--	-33.56
193	1.09	1.09	0.00	0.10	1.09	0.00	0.10	1.00	-0.36	--	-0.33
194	5.18	3.41	1.77	0.18	3.48	1.70	0.50	1.15	-2.06	3.98	-171.37
195	3.63	3.01	0.63	0.15	3.08	0.55	0.45	1.05	-2.41	12.26	-203.03
196	2.68	2.68	0.00	0.13	2.68	0.00	0.34	1.00	0.09	--	-157.09
197	1.93	1.93	0.00	0.11	1.93	0.00	0.13	1.00	0.22	--	-22.16
198	2.49	0.71	1.77	0.16	0.76	1.73	0.50	0.25	-6.69	2.53	-219.66
199	1.92	0.62	1.30	0.14	0.62	1.32	0.48	0.20	0.14	-1.81	-253.59
200	0.90	0.90	0.00	0.15	0.90	0.00	0.09	1.00	-0.27	--	41.18
201	3.29	1.98	1.31	0.15	1.95	1.34	0.48	0.65	1.65	-2.21	-224.14
202	2.57	1.95	0.61	0.13	1.91	0.61	0.46	0.65	2.17	0.65	-254.07
203	1.56	1.56	0.00	0.09	1.56	0.00	0.12	1.00	0.26	--	-26.65
204	2.45	0.71	1.74	0.15	0.76	1.69	0.49	0.25	-6.68	2.75	-218.01
205	1.90	0.60	1.29	0.14	0.60	1.30	0.48	0.20	0.65	-0.49	-252.08
206	0.65	0.65	0.00	0.16	0.65	0.00	0.07	1.00	0.16	--	54.84
207	3.19	1.71	1.49	0.16	1.80	1.39	0.48	0.60	-5.54	6.45	-197.37
208	2.53	1.98	0.55	0.14	2.05	0.48	0.45	0.70	-3.30	12.03	-232.72
209	1.60	1.60	0.00	0.10	1.60	0.00	0.12	1.00	0.07	--	-21.01
210	1.28	1.28	0.00	0.09	1.28	0.00	0.11	1.00	0.27	--	-22.22
211	3.21	1.23	1.98	0.15	1.21	2.68	0.25	0.50	1.52	-35.32	-72.02
212	2.49	1.19	1.30	0.13	1.16	1.76	0.21	0.50	2.13	-35.09	-61.13
213	3.35	0.84	2.51	0.34	0.87	1.64	0.27	0.35	-4.11	34.73	19.46
214	2.57	0.72	1.85	0.13	0.72	1.25	0.24	0.30	0.04	32.40	-85.09
215	3.24	1.28	1.96	0.14	1.21	1.36	0.25	0.50	5.39	30.62	-76.61
216	2.50	1.26	1.24	0.13	1.27	0.91	0.21	0.55	-0.44	26.35	-63.64
217	3.25	1.85	1.40	0.15	1.86	0.95	0.22	0.80	-0.49	32.21	-49.66
218	2.37	1.46	0.91	0.13	1.50	0.87	0.20	0.65	-2.93	4.88	-59.86

Table 15: Continued.

	Observed Values				Simulated Values				Performance Bias		
Experiment Number	**Q_A (cfs)**	**Q_I (cfs)**	**Q_O (cfs)**	**D_A (ft)**	**Q_I-Link 7 (cfs)**	**Q_O-Link 4 (cfs)**	**D_A-Link 1 (ft)**	**Coefficient**	**Inlet Bias**	**Outlet Bias**	**Depth Bias**
219	3.59	1.78	1.81	0.15	1.82	1.77	0.50	0.60	-2.28	2.18	-239.17
220	3.08	2.62	0.46	0.14	2.63	0.45	0.45	0.90	-0.33	1.36	-211.42
221	1.83	1.83	0.00	0.11	1.83	0.00	0.13	1.00	-0.03	--	-20.37
222	1.40	1.40	0.00	0.10	1.40	0.00	0.11	1.00	-0.25	--	-12.44
223	2.20	0.48	1.72	0.15	0.45	1.75	0.50	0.15	6.04	-1.58	-239.75
224	1.84	0.56	1.28	0.15	0.60	1.24	0.48	0.20	-7.64	3.28	-230.65
225	0.67	0.67	0.00	0.12	0.67	0.00	0.07	1.00	0.57	--	40.17
226	2.20	0.48	1.72	0.15	0.45	1.75	0.50	0.15	6.04	-1.58	-239.75
227	1.79	0.41	1.38	0.13	0.45	1.34	0.48	0.15	-8.67	2.86	-275.98
228	0.34	0.34	0.00	0.16	0.34	0.00	0.05	1.00	-0.64	--	68.15
229	2.98	1.40	1.58	0.16	1.36	1.62	0.49	0.45	2.74	-2.56	-201.23
230	2.08	0.91	1.17	0.14	0.90	1.18	0.48	0.30	1.15	-0.84	-253.37
231	1.19	1.19	0.00	0.10	1.19	0.00	0.10	1.00	0.04	--	-1.81
232	1.46	1.46	0.00	0.10	1.46	0.00	0.11	1.00	-0.34	--	-13.50
233	3.63	1.29	2.34	0.14	1.24	3.23	0.27	0.50	3.97	-37.86	-90.14
234	2.80	1.38	1.42	0.13	1.40	0.96	0.22	0.60	-1.12	32.38	-65.00
235	3.06	1.00	2.06	0.13	0.97	1.40	0.25	0.40	3.38	31.98	-92.14
236	2.48	0.58	1.90	0.14	0.60	1.27	0.24	0.25	-3.57	33.30	-75.75
237	3.17	0.49	2.68	0.15	0.80	1.76	0.28	0.20	-63.38	34.37	-84.75
238	2.21	0.26	1.94	0.14	0.24	2.64	0.24	0.10	8.50	-35.87	-75.75
239	3.52	1.73	1.78	0.16	1.68	1.24	0.25	0.70	2.92	30.52	-58.79
240	2.75	1.68	1.07	0.14	1.68	0.90	0.21	0.70	0.10	15.74	-54.66
241	3.87	2.09	1.78	0.18	2.12	1.75	0.50	0.70	-1.35	1.49	-176.78
242	3.17	1.97	1.20	0.17	1.95	1.22	0.48	0.65	0.81	-1.37	-187.43
243	2.11	2.11	0.00	0.12	2.11	0.00	0.14	1.00	0.18	--	-15.46
244	1.35	1.35	0.00	0.10	1.35	0.00	0.11	1.00	0.24	--	-11.68
245	3.59	2.11	1.48	0.15	2.11	1.48	0.49	0.70	0.04	0.17	-230.71
246	2.96	2.06	0.91	0.14	2.08	0.89	0.47	0.70	-1.06	1.78	-242.03
247	1.97	1.97	0.00	0.11	1.97	0.00	0.13	1.00	-0.11	--	-14.54
248	2.01	2.01	0.00	0.11	2.01	0.00	0.14	1.00	-0.09	--	-22.09

Table 15: Continued.

	Observed Values				Simulated Values				Performance Bias		
Experiment Number	**Q_A (cfs)**	**Q_I (cfs)**	**Q_O (cfs)**	**D_A (ft)**	**Q_I-Link 7 (cfs)**	**Q_O-Link 4 (cfs)**	**D_A-Link 1 (ft)**	**Coefficient**	**Inlet Bias**	**Outlet Bias**	**Depth Bias**
249	5.20	3.80	1.40	0.18	3.90	1.30	0.49	1.30	-2.61	7.22	-173.36
250	4.96	4.04	0.92	0.20	4.01	0.95	0.47	1.50	0.79	-3.06	-132.00
251	3.57	3.57	0.00	0.15	3.57	0.00	0.37	1.30	0.10	--	-151.42
252	2.57	2.57	0.00	0.13	2.57	0.00	0.29	1.00	0.12	--	-126.71
253	5.17	3.71	1.46	0.18	3.76	1.41	0.49	1.25	-1.36	3.36	-178.94
254	4.23	3.41	0.82	0.15	3.40	0.82	0.47	1.15	0.30	-0.56	-203.55
255	2.78	2.78	0.00	0.13	2.78	0.00	0.38	1.00	0.04	--	-187.33
256	1.79	1.79	0.00	0.11	1.79	0.00	0.13	1.00	0.16	--	-19.82
257	3.37	1.25	2.12	0.17	1.22	2.15	0.51	0.40	2.50	-1.31	-196.94
258	2.27	0.84	1.43	0.15	0.90	1.36	0.48	0.30	-7.55	4.83	-220.18
259	0.52	0.52	0.00	0.13	0.52	0.00	0.06	1.00	-0.37	--	54.89
260	2.47	0.70	1.77	0.15	0.76	1.72	0.49	0.25	-8.30	2.95	-222.37
261	2.15	0.76	1.39	0.15	0.75	1.40	0.48	0.25	0.96	-0.38	-213.88
262	0.84	0.84	0.00	0.20	0.84	0.00	0.08	1.00	-0.37	--	58.97
263	3.00	0.86	2.14	0.14	0.86	1.43	0.25	0.35	-0.03	33.03	-76.06
264	2.14	0.59	1.55	0.12	0.59	2.07	0.21	0.25	-0.76	-33.13	-72.60
265	3.87	1.84	2.03	0.15	1.82	2.03	0.26	0.75	1.33	-0.03	-73.72
266	3.20	1.98	1.22	0.14	2.10	0.96	0.22	0.90	-6.08	21.01	-58.27
267	5.01	3.52	1.49	0.18	3.52	1.62	0.25	1.50	0.00	-8.74	-40.45
268	4.25	3.07	1.18	0.16	3.01	0.92	0.23	1.30	2.03	21.70	-44.65
269	6.61	5.58	1.03	0.21	5.52	1.09	0.48	1.85	1.00	-5.68	-131.51
270	3.89	3.89	0.00	0.15	3.89	0.00	0.39	1.40	0.09	--	-161.16
271	3.68	2.05	1.63	0.15	1.97	1.71	0.50	0.65	4.03	-5.01	-241.69
272	2.24	2.24	0.00	0.12	2.24	0.00	0.18	1.00	-0.10	--	-48.35
273	2.26	0.61	1.65	0.12	0.61	1.65	0.49	0.20	-0.70	0.14	-308.33
274	1.15	1.15	0.00	0.14	1.15	0.00	0.10	1.00	0.27	--	29.58
								Average Bias	-0.23	1.64	-66.52